

Microfabricated Probiotic Formulation for Inhibition of Salmonella in Poultry

by

Manika Chopra

A thesis submitted in partial fulfillment of the requirements for the degree of

Master of Science

in

Chemical Engineering

Department of Chemical and Materials Engineering
University of Alberta

© Manika Chopra, 2020

Abstract

Salmonella is a major pathogenic bacteria found in both animals and humans. It leads to one of the most common foodborne diseases and is often transmitted to humans through the consumption of animal products. Antibiotics have long been used in the agriculture industry to prevent and treat *Salmonella* infections, but their use has come under major scrutiny with the recent emergence of antibiotic-resistant bacteria. This has increased the awareness of the benefits of probiotics, especially with regards to their antimicrobial activity. Furthermore, their acceptance as an alternative treatment option to antibiotics is largely due to their natural occurrence in the microbiota of hosts. In this context, and according to current definitions, probiotics must be delivered as “live” cells, which is a significant concern in pharmaceutical industries due to the inherent loss of cells as a result of the harsh conditions of the digestive tract. Often times, formulations will contain larger amounts of cells than effective dose requirements to make up for cells lost during administration, making the process inefficient and increasing costs for manufacturing. In this study, we successfully demonstrated the formulation of a delivery system that protected the viability of the probiotic *Lactobacillus acidophilus* for application in poultry feed to inhibit *Salmonella*.

Micromilling was used to design a delivery system, and micro-mold casting technology was incorporated to fabricate a solid formulation. Process parameters and procedures – such as encapsulation formulation, drying time, and spray coating thickness – were optimized using Sulforhodamine B as a model drug. The protective efficacy and release characteristics of the system with EUDRAGIT® S 100 polymer was determined by conducting in vitro digestive tests using Sulforhodamine B dye. The release rate of encapsulated Sulforhodamine B dye in the optimized system was measured to be 0.251%/ min of exposure to simulated gastric fluid. Only

10 ± 8 % of dye was leaked during incubation in simulated gastric fluid. Successful release of the encapsulated agent was observed upon addition to neutral simulated intestinal fluid, showing the pH responsive abilities of the system. The protein concentration contained in a single patch encapsulating *L. acidophilus* was determined to be 34.2 ± 13.2 µg. The formulation and S100 polymer showed no negative effects on viability of encapsulated *L. acidophilus* cells and proved to protect the cells during *in vitro* tests. More specifically, the cell viability after exposure to harsh digestive conditions was 5.2 times higher, and the inhibition zone against *Salmonella* was 9.5 % larger with the application of the S100 spray coated polymer. Short term environmental stability tests showed minimal degradation of cells and the protective abilities of the polymer and formulation were once again observed during *in vitro* studies. Additionally, the S100 polymer likely protected the cells from hydrolytic degradation due to humidity, which could be applied during commercialization stages to fulfill packaging requirements.

This work is the starting point for future developments in micro-fabricated oral drug delivery systems. The unique structure of this system can be further investigated for co-delivery of other agents. Additionally, the formulation could also be optimized to limit the degradation of *L. acidophilus* cells during long-term storage to improve the efficacy of probiotics and ensure successful commercialization of the system.

Acknowledgements

I would like to acknowledge my supervisors, Dr. Hyo-Jick Choi and Dr. Dominic Sauvageau for this opportunity, along with their support and guidance throughout my degree. I have learned so much from the both of you at both the professional and personal level, and I know this experience would not have been the same without you both. Thank you for teaching me how to push past my limit and to think outside of the box, you have shaped me into a better learner.

Thank you to all my lab mates in both Dr. Choi and Dr. Sauvageau's group. I feel so fortunate to have been surrounded by such inspirational people, and I am so grateful to every single one of you for all of your help throughout this journey. Special thanks to Surjith, Harish, Ilaria, and Bahman for all of your help at the beginning of my journey and for always being there to motivate me, to Dilini and Jashan for taking your time to help me with more than just my experiments, to Euna for teaching me fundamental research skills and always being available to answer any of my biology questions, and to Sumin for turning off the sonicator for me on multiple occasions and being such a positive friend. I would also like to thank Ana for taking the time to discuss phages, to Bea for all of the phages training and thesis help, and to Miranda for all of the support with my thesis and being a mentor/friend even outside of the lab.

A very special thank you to all of my friends that I knew before grad school and to the lifelong friends I have made during this journey. I am so thankful for your support and encouragement even at the hardest of times.

I am immensely grateful for the love and support from my family. To my mom and dad, I can confidently say that I could not have done this without you. You have both taught me the most important values in life, supported and encouraged me throughout my education, and given me the

most love in the world. To my sister, brother-in-law, and nephews, Zavian and Aarav, thank you for being the biggest distraction to my thesis, your love and presence was worth all the stress. Thank you Nani for always making my favorite foods to fuel my brain and Dadu for all the unconditional love every day. Lastly, Jasin, your work ethic is unmatched and has taught me to persevere even in the toughest of times. Thank you for being such a lighthearted and supportive pillar throughout my degree, you've been my biggest fan from day one.

Table of Contents

1. Introduction	1
2. Literature Review	2
2.1 Salmonella	2
2.1.1 Pathogenesis	3
2.1.2 Mitigation Methods	4
2.2 Probiotics	5
2.2.1 Classification	6
2.2.2 Mechanism	7
2.2.3 Poultry	11
2.2.4 Technical Challenges and Applications of Current Probiotic Formulations	12
3. Project design and hypotheses	18
4. Materials and Methods	19
4.1 Aluminum master mold and PLA/PDMS casting mold fabrication	19
4.2 Bacterial cell culture	21
4.3 Fabrication of probiotics patch	22
4.4 Spray coating	24
4.5 Characterization of cell viability during fabrication process	26
4.6 Stability in simulated digestive conditions	27
4.6.1 Dye release tests:	28
4.6.2 Environmental stability test:	28
4.7 Characterization	29
4.7.1 Colony Forming Units (CFU)	29
4.7.2 Agar well diffusion test	29
4.7.3 Protein concentration	30
4.7.4 Optical microscopy	30
4.8 Statistical analysis	31
5. Results and Discussion	31
5.1 Mold Fabrication	31
5.2 Effect of Fabrication Process on Cell Viability	34
5.3 SB Dye Release Test	41

5.4 Formation of a Protection Layer via Spray Coating of S100 Anionic Copolymers	42
5.5 Release Behavior of the Patch with a Protection Layer in Simulated Digestive Conditions of Poultry	45
5.6 Preservation and Delivery of <i>L. acidophilus</i> in Simulated Digestive Conditions	49
5.7 Environmental Stability Test of <i>L. acidophilus</i>	55
6. Conclusions and Future Work.....	59
References	62

List of Figures

Figure 1. The structure of the Type 3 Secretion System (T3SS) of <i>Salmonella</i> associated with virulence. Image adapted from [13]......	4
Figure 2. Antibacterial mechanisms of probiotics. Image adapted from [71].	8
Figure 3. Bacteriocin pore forming mechanisms (a) barrel-stave, (b) thoroidal, and (c) carpet models. Image from [37]......	10
Figure 4. Three different ways for encapsulation of probiotics. Image from [50].	14
Figure 5. Comparison of spherical and planar microparticle for adhesion to epithelium lining. Image from [57].	16
Figure 6. Fabrication steps for polymer molding. Image from [62].	17
Figure 7. Fabrication with a micromilling machine. (a) Computer aided design, (b) simulation, (c) CNC machine, and (d) live image of fabrication.	21
Figure 8. Schematic representation of the probiotic patch fabrication process.	24
Figure 9. Spray coating process set up.....	26
Figure 10. Aluminum master structure. (a) Before smoothing, (b) after smoothing, and (c) SEM image of a negative PDMS mold from the aluminum master structure after smoothing. Inset image represents a high magnification image where scale bar is 500 μm	33
Figure 11. <i>L. acidophilus</i> cell viability. (a) Cell stability in a suspension of DI and trehalose for various incubation periods at RT, and (b) the effect of corresponding process incubation periods at 37 °C on cells encapsulated in a PDMS mold. The mean value was calculated from 3 replicates and the error bars indicate standard deviation. Note: ** p-value > 0.05 by ANOVA. 35	
Figure 12. Schematic representation of the probiotic patch fabrication process. Note: * Molded w/o backing, ** Molded w/o backing MRS, *** Demolded w/ backing MRS.	36
Figure 13. Change in cell viability of samples, i) molded without a CMC backing and ii) demolded with a CMC backing, with the increase of incubation time in MRS broth ((a) 6 hours, (b) 12 hours, (c) 24 hours, and (d) 48 hours). The mean value was calculated from 3 replicates and the error bars indicate standard deviation.	38
Figure 14. Cell viability of samples incubated in MRS broth for 48 hours i) molded without a CMC backing, and ii) demolded with a CMC backing in comparison to iii) molded without a CMC backing and directly measured without incubation in MRS broth. The mean value was calculated from 3 replicates and the error bars indicate standard deviation.	40

Figure 15. Fluorescent images of SB dye encapsulated molds release behavior. (a) Before and (b) after exposure to DI for 90 seconds.	42
Figure 16. SEM images of a spray coated silicon wafer after (a) 2 seconds of coating, (b) 5 seconds of coating, and (c) 10 seconds of coating (i: cross-sectional view, ii: top view). Note: PC is polymer coating on top of the silicon wafer.....	43
Figure 17. Protection layer thickness as a function of spray coating time. The linear equation for the coating rate was $y = 1.076 \cdot x$. Error bars indicate the standard deviation as calculated by the SEM analysis in Table 2.	44
Figure 18. <i>In vitro</i> release test of SB dye encapsulated in molds spray coated for (a) 2 seconds, (b) 5 seconds, and (c) 10 seconds. The mean value was calculated from 3 replicates and the error bars indicate standard deviation.....	47
Figure 19. Release of SB dye as a function of time in SGF of molds spray coated for (a) 2 seconds, (b) 5 seconds, and (c) 10 seconds. The linear equation is seen on each plot, where R is the release rate (%) and t is the time exposed to SGF (min). The mean value was calculated from 3 replicates and the error bars indicate standard deviation.	48
Figure 20. Release of SB dye in simulated gastric conditions as determined by experimental release rate equations for various periods of time a sample is spray coated. Error bars indicate the standard deviation as determined by the linear regression from Figure 19.	49
Figure 21. Time-dependent cell growth of <i>L. acidophilus</i> in simulated digestive conditions after incubation in MRS broth for (a) 12 hours, (b) 24 hours, and (c) 48 hours. Note: * CFU/mL < 500. The mean value was calculated from 3 replicates and the error bars indicate standard deviation.....	51
Figure 22. <i>L. acidophilus</i> cell viability after exposure to simulated digestive conditions and incubation in MRS broth for 48 hours. (a) Batch #1, (b) Batch #2, (c) Batch #3, and (d) all batches combined. The mean value was calculated from 3 replicates and the error bars indicate standard deviation for all except for (d) where the mean and standard deviation were calculated from the 3 batches. In Figure (d), * P < 0.05 and ** P > 0.05 by ANOVA.	53
Figure 23. Sealing of samples for stability tests. (a) Patch encapsulated with SB dye in a pill bottle, (b) Sealing of bottles foil seal using electromagnetic induction sealer, (c) Visual confirmation of successful sealing of foil, and (d) Removal of foil seal from bottle.	57
Figure 24. Environmental stability of cells upon exposure to digestive conditions after storage at 37 °C and 70 % RH for 1 day and 1 week. The mean value was calculated from 3 replicates and the error bars indicate standard deviation. * P < 0.05 and ** P > 0.05 by ANOVA.....	58

List of Tables

Table 1. Stability test conditions.....	29
Table 2. Protection layer thickness according to SEM image analysis	44
Table 3. Agar well diffusion inhibition zone produced by <i>L. acidophilus</i> against <i>S. typhimurium</i> . The mean value and standard deviation were calculated from 3 replicates.....	55
Table 4. Environmental Stability Test Conditions.....	58

Table 5. Agar well diffusion inhibition zone diameters for samples upon exposure to digestive conditions after being stored at 37 °C and 70 % RH for 1 day and 1 week. The mean value and standard deviation was calculated from 3 replicates..... 59

1. Introduction

Antibiotics have played a large role in inhibiting the growth or killing bacteria in clinical settings since their introduction in the 1930s [1]. They continue to be used for the treatment and prevention of infections in a wide range of living organisms, from humans to plants and animals. The use of antibiotics has transformed the development of society, having allowed for significant growth in the medical field and agriculture industry. For example, it is reported that approximately 80% of all antibiotics in the USA are used for livestock [2].

Antibiotic use is multifaceted in agricultural settings where it is utilized to treat/ prevent diseases, such as Salmonellosis, and to improve feed conversion efficiency to promote growth of livestock [3]. For poultry, antibiotics are normally administered orally by addition to drinking water and feed, and the average amount of antimicrobial agent consumed per annum of animal produced is 148 mg/kg [4]. However, since broiler chickens are often confined in cages together and since food consumption will vary between them, it has been a challenge to control the dosage of antibiotics administered to each animal [5]. As a result, healthy animals tend to consume more food, and thus antibiotics, than sick animals, raising concerns about the efficacy of this approach to treatment.

The evolution of multidrug-resistant (MDR) bacteria has emerged as another major issue resulting from antibiotic use [1]. MDR bacteria such as *Salmonella typhimurium* are resistant to antibiotics that are traditionally used to treat them, requiring more specific or restricted care and possibly multiple drug cocktails for treatment instead [3]. More importantly, this can lead to the generation of a multiple-drug-resistant strain, such as the totally drug resistant *Tuberculosis bacilli* [6]. This is a significant concern as approximately 23,000 annual deaths in the USA are attributed to antibiotic-resistant infections [2].

Antibiotic-resistant bacteria are a result of the consumption and misuse of antibiotics in clinical and agricultural settings. Antibiotics used to produce animal products for human consumption have shown to also contribute to the rise in antibiotic-resistant bacteria [5]. Similar to humans, animals can develop antibiotic-resistant bacteria due to the overconsumption of antibiotics, resulting in cross-species transmission to humans. This transmission can take place through direct or indirect contact between the species, especially through food or shared environments [7]. Moreover, the presence of antibiotic residues on animal products can have adverse toxicity effects on human health [5]. The increasing awareness of adverse consequences associated with antibiotic-resistant bacteria has driven the development of alternative technologies (e.g., the use of probiotics instead of antimicrobial agents) to minimize or even eliminate the use of antibiotics.

2. Literature Review

2.1 Salmonella

The US Centers for Disease Control and Prevention (CDC) estimates that there are 48 million cases and 3,000 deaths as a result of foodborne illnesses each year in the United States. Amongst 250 foodborne diseases, *Salmonella* is listed as one of the top five most common bacteria to cause illness [8]. *Salmonella* is a Gram-negative bacterium found in both humans and animals. *Salmonella enterica* subsp. *enterica* is responsible for 99% of infections in warm-blooded animals, with the serotype *S. typhimurium* causing most gastrointestinal infections in humans [9]. A range of illnesses are attributed to *Salmonella* infection, such as enteric fever, bacteremia, enterocolitis, and focal infections [10].

2.1.1 Pathogenesis

In spite of the risk of person-to-person transmission of *Salmonella*, the main method of pathogenesis for humans is through the consumption of contaminated food, especially through beef, poultry, and eggs [10], [11]. According to a report by Darwin and Miller (1999), approximately 10^5 - 10^{10} bacteria are needed to initiate an infection, depending on the strain [10]. The bacterium is able to pass into the intestine where it adheres to the intestinal epithelium and enters the cells that line it. The invasion of *Salmonella* in the intestine triggers an influx of neutrophils, causing inflammation in the tissue. People with *Salmonella* infection develop symptoms such as diarrhea, nausea, vomiting, cramping, and fever. In addition, various serotypes may spread to other organs in the body, such as the liver, spleen, gall bladder, etc. [12].

Like many other pathogens, *Salmonella* depends on the Type-Three Secretion System (T3SS; Figure 1) to invade, colonize and destruct cells [13]. The T3SS has been researched extensively due to the large role it plays in understanding bacterial pathogenesis and bacteria-host interactions. Approximately 20 proteins make up the entire T3SS structure, which can be categorized into structural, translocator, and effector proteins. Structural proteins form a needle like structure with two rings, one that crosses the inner membrane and another that crosses the outer membrane of the cell. Once the needle structure attaches to the host, translocator proteins are secreted to create pores in the host cell membrane, from which effector proteins are transported into the host cell cytoplasm [14], [15]. It is hypothesized that a signal mechanism is used to ensure that the T3SS is only deployed when the bacterium comes into contact with the target host cell, and not prematurely [16]. The effector proteins help *Salmonella* invade nonphagocytic cells in the epithelium to form a *Salmonella*-containing vacuole, which allows for the survival and colonization of *Salmonella* in the host. The disruption of the epithelial barrier by *Salmonella* is

thought to induce chloride secretion in the epithelium, resulting in diffusion of water and one of the most common symptoms of *Salmonella* infection, diarrhea [17]. Effector proteins also have the ability to inhibit the host immune responses through interaction with the host cell proteins, or by creating an environment to protect from cellular killing, enabling the further spread and persistence of *Salmonella* in the host [14].

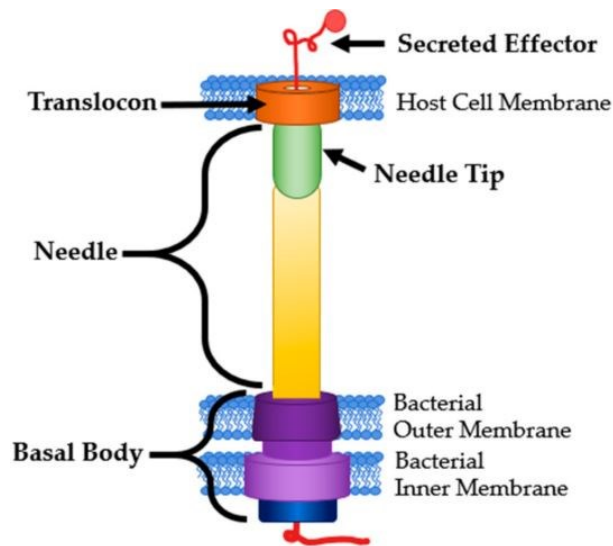


Figure 1. The structure of the Type 3 Secretion System (T3SS) of *Salmonella* associated with virulence. Image adapted from [13].

2.1.2 Mitigation Methods

Foodborne *Salmonella* is a major source for human infection and carries a heavy financial burden on the agriculture industry [18]. Thus, many control measures have been used to limit the transmission of *Salmonella*, especially in poultry. Poultry husbandry practices have been shown to impact *Salmonella* colonization, with overcrowding of cages being a major factor [19]. *Salmonella*-monitoring regulations, such as the National Antimicrobial Monitoring System program, have been implemented to identify and control outbreaks in animals during primary production; but these often only minimize the impact of the disease instead of preventing the initial

outbreak. Vaccines have also been used in conjunction with monitoring regulations; however, no currently available vaccine protects against all *Salmonella* serogroups. Thus, the efficacy of vaccines is debatable for the moment, as there is concern over the potential further aggravation of the prevalence of emerging serotypes [19]. On the other hand, antibiotics, such as fluoroquinolones, have often been used to prevent *Salmonella* and promote growth in poultry production. However, since the overuse of antibiotics in poultry has been shown to play a role in the transmission of MDR *Salmonella* to humans, there are major concerns over its usage in agriculture [20]. Bacteriophages and phage therapy were discovered a decade before the first antibiotic, penicillin. Unlike antibiotics, they have the ability to target and infect specific bacterial species or strain [21]. Although phage therapy has been around for over a century, the discovery of antibiotics shifted the focus away from phages and towards antibiotics. Now that Western medicine is beginning to realize the adverse side effects of antibiotics, more specifically the evolution of MDR bacteria due to antibiotics, phage therapy and biocontrol in poultry has been the subject of many recent studies [22], [23], [24].

2.2 Probiotics

The word “probiotic” was coined in 1974 and is defined by the World Health Organization as “live microorganisms which when administered in adequate amounts confer a health benefit to the host” [25] [26]. The history of probiotics goes back well before the name was developed, with Sumarian paintings showing indications of lactic acid fermentation of milk, which is a source of probiotics, as early as 2500 B.C. [25]. “Probiotics” has recently become a buzz word in main stream media for health and well-being, but Elie Metchnikoff was one of the first to promote probiotics for therapeutic use in his book “*Essais Optimistes*” published in 1907. Many of the

medical concepts defended in this work still hold true today, such as the connection between chronic disabilities and intestinal health, and enhancement of health through manipulation of the intestinal microbiome [27]. Metchnikoff focused on the strain “Bulgarian bacillus”, which is now known as *Lactobacillus bulgaricus*, as he found that Bulgarian peasants consuming large amounts of soured milk lived longer lives [25]. Metchnikoff was awarded the Nobel Prize for his work in immunology, but his concepts related to probiotics only began to gain traction in the mid-1990s, and are now the source of the multi-billion dollar global industry we see today in food and pharmaceuticals [27].

2.2.1 Classification

Lactic acid bacteria (LAB) are members of the Lactobacillales order of the Firmicutes, with 6 families, more than 30 genera and over 300 species [28]. It is generally accepted that they belong to the Gram-positive phylum with a low G+C content (<50%), are non-spore forming and either coccobacilli or rods [29]. The genus *Bifidobacterium* also falls within the LAB designation but belongs to the phylum Actinobacteria. This shows how LAB classification may not always follow traditional classification methods. The most common genera found in probiotics are *Enterococcus*, *Bifidobacterium*, and *Lactobacillus*, which will be the main focus of this work [30].

Lactobacillus species are commonly found in a number of fermented foods, such as wine, breads, fruits and vegetables, dairy, etc., and are known constituents of the gastrointestinal and vaginal tracts of humans/animals. Since there is such a large number of *Lactobacillus* species with a wide range of biochemical and physiological properties, multiple species were initially identified incorrectly and have had to be reclassified over the years. As a result, phenotypic and genotypic data can be integrated, otherwise known as polyphasic taxonomy, to develop a classification

framework for the taxonomy of *Lactobacillus*. Genomic sequencing comparisons with 16 sRNA, rep-PCR, or pulsed-field gel electrophoresis can be used with phenotypic characterization, such as sugar fermentation patterns, to identify species and strains [31].

According to their fermentation pathways, *Lactobacillus* can be classified into three main groups: obligatory homo-fermentative, facultative hetero-fermentative, or obligatory hetero-fermentative. Obligatory homo-fermentative LAB produce lactic acid as a major end product, but may produce formic acid when under stress conditions. They use the Embden-Meyerhof-Parnas (EMP) pathway. The most common homo-fermentative LAB are *Lactobacillus acidophilus*, *Lactobacillus bulgaricus*, and *Lactobacillus helveticus*. Similarly, facultative hetero-fermentative LAB can ferment hexose to lactic acid by the EMP pathway. They can also i) produce co-products, like ethanol and/or acetic acid, in addition to lactic acid under glucose limitations, and ii) ferment pentose, as they have the enzymes aldolase and phosphoketolase. Examples of facultative hetero-fermentative LAB include *Lactobacillus plantarum*, *Lactobacillus casei*, and *Lactobacillus sake*. Lastly, obligatory hetero-fermentative bacteria also produce co-products, like CO₂, ethanol, and/or acetic acid, in addition to lactic acid. However, hexose is fermented using the phosphogluconate pathway instead, and pentose may enter this pathway and also be fermented. Examples of obligatory hetero-fermentative LAB include *Lactobacillus brevis*, *Lactobacillus fermentum*, and *Lactobacillus reuteri* [32].

2.2.2 Mechanism

Lactobacilli thrive in environments rich in carbohydrate-containing substrates, such as the oral cavity and intestine of humans/ animals. Their beneficial health effects on organisms are often seen in the gastrointestinal (GI) tract, especially in inhibiting pathogenic bacteria such as

Salmonella. There are three main mechanisms (Figure 2) in which probiotics may be beneficial in the GI tract: i) antagonism due to the production of their antimicrobial substances, ii) competition with pathogens to adhere to epithelium, and iii) immunomodulation of the host [33].

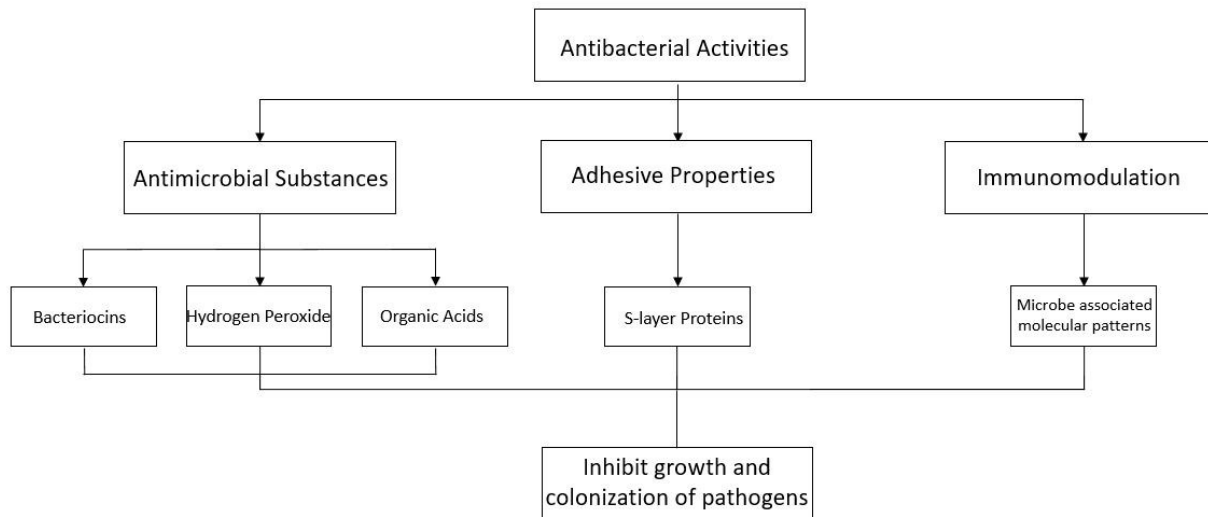


Figure 2. Antibacterial mechanisms of probiotics. Image adapted from [77].

According to Monteagudo et al. (2018), competition with pathogens to adhere to the intestinal tract does not directly correlate to the inhibition of pathogens, but instead acts as a protective barrier to the host to mitigate the colonization of pathogens by competing over binding sites. The adhesion to the intestinal epithelial is attributed to the presence of mucous binding proteins and pili on the *Lactobacillus* cell. The mucosa layer of the epithelium consists mainly of mucin, which is the anchor for mucin binding proteins on the *Lactobacillus* cell wall to adhere to the epithelium. Other surface proteins, such as fibronectin-binding proteins, or surface layer proteins, such as choline-binding protein A, have also been shown to assist in the binding abilities of *Lactobacillus* [34].

Pattern recognition receptors (PRRs) are proteins present on the epithelial cell membrane that have the ability to recognize molecules associated with the endogenous microbiota of the host and pathogens, called microbe-associated molecular patterns (MAMPs) and pathogen-associated molecular patterns (PAMPs), respectively [35]. There are many mechanisms in which MAMPs contribute to immunomodulation, for example the suppression of pro-inflammatory cytokines, such as tumour necrosis factor alpha (TNF- α) and interleukin (IL-7). Probiotics, through this defense mechanism, are thought to be effective at alleviating symptoms of immune-associated diseases, like inflammatory bowel diseases [34].

One of the best-known antibacterial mechanisms of *Lactobacillus* is their ability to produce inhibitory substances, such as bacteriocins, hydrogen peroxide, and organic acids. Bacteriocins are proteins produced by bacteria that are potent to other bacterial strains. There are four groups of bacteriocins produced by LAB that are differentiated according to their molecular weights and genetic characteristics. Class I contains post-translationally modified bacteriocins that are less than 5 kDa and are called lantibiotics. Class II bacteriocins are heat stable, unmodified and their size is less than 10 kDa. These can be further divided into two groups according to their need for a secondary peptide to activate their antimicrobial activity. Class III bacteriocins are heat labile unmodified proteins larger than 30 kDa [29]. Bacteriocins are released as a consequence of a lysed cell or actively secreted from a cell. They contain a transporter gene in order to cross through the cell membrane and reach a pathogenic cell. Immunity genes ensure that its own cell is protected against the antagonist activity of the bacteriocins. Once the bacteriocin has reached the target membrane, electrostatic interactions between the amino acid groups of the bacteriocin and phospholipids of the membrane drive the binding mechanism [36]. After binding with the target membrane, the bacteriocin produces a pore according to a barrel-stave, toroidal, or carpet model

[37]. The formation of a pore in the target membrane results in the leakage of essential compounds for cell function, including cations. Furthermore, this leakage of cations disrupts the proton motive force, inducing cell death [36].

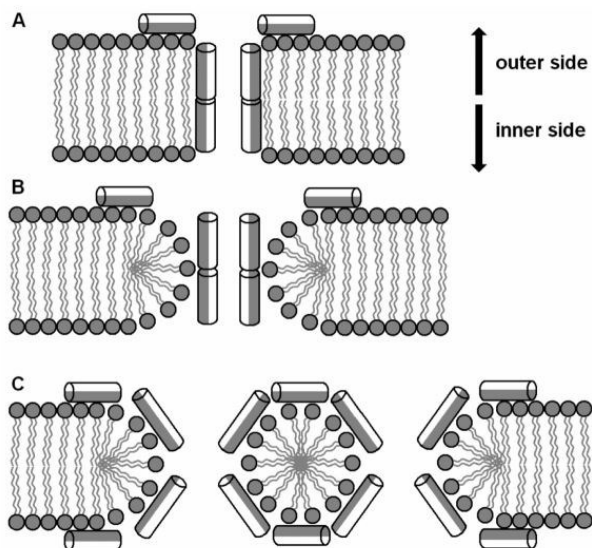


Figure 3. Bacteriocin pore forming mechanisms (a) barrel-stave, (b) toroidal, and (c) carpet models. Image from [37].

Similarly to bacteriocins, organic acids also have the ability to dissipate the proton motive force. As discussed previously, lactic acid is usually the main metabolic product from carbohydrate fermentation regardless of the fermentation pathway used, and acetic acid may also be produced. In their non-dissociated form, lactic and acetic acids have the ability to penetrate into Gram-negative bacteria through porin proteins found on the outer membrane. The nearly neutral pH of the cytoplasm of the target bacteria results in the dissociation of the acid to produce hydrogen ions, which accumulate in the cell and reduce the intracellular pH. The presence of hydrogen ions interferes with metabolic functions and impacts the proton motive force. The antimicrobial activity of each of the acids depends on the pH and their dissociation constant. At an external pH below

the dissociation constant, the acid that has the higher dissociation constant will have more non-dissociated acid, thus a stronger antimicrobial effect upon permeating the cell [32] [38].

Hydrogen peroxide has been known as natural disinfectant or preservative, and is still used today, especially as a disinfectant for clothing and surfaces [39]. Lactobacilli produce excess amounts of hydrogen peroxide as they convert oxygen using nicotinamide adenine dinucleotide (NAD) [40]. The antimicrobial activity of hydrogen peroxide relies on its ability to reduce to hydroxyl radicals, which are able to attack the membrane lipids, DNA, and other cellular components of the target bacteria [39]. *Lactobacillus* has the ability to remove hydrogen peroxide by reacting with NADH peroxidase, producing only water. Thus, no hydroxyl radicals are produced, limiting its effect on *Lactobacillus* [40]. Interestingly, hydrogen peroxide has been shown to have a higher inhibition against Gram-negative bacteria, like *Salmonella* [39].

2.2.3 Poultry

The GI tract of poultry is much shorter than other mammals with similar body lengths. Despite this, it is host to a wide diversity of bacteria, with anywhere between $10^5 - 10^{12}$ bacteria cells per gram of luminal content depending on the location in the tract [41]. The main components of the GI tract are the esophagus, crop, proventriculus and gizzard, small intestine, caeca, and cloaca. The crop is a sac-like organ that is connected to the esophagus. Depending on the feeding pattern of the animal, the crop can be used as a storage pouch for feed, or the food may bypass the crop and continue through the esophagus to the proventriculus. There is no degradation of the feed in the crop, thus the pH of the feed remains constant while stored there. Svihus (2014) described how the proventriculus and gizzard act as the stomach. The proventriculus is the first section, where enzymes are secreted to begin the digestion process, decreasing the pH to 1.9 - 4.5, with an

average of approximately 3.5. Then, the food moves to the gizzard, where the strong muscles and the sandpaper-like surface grind the feed and mix it with the digestive juices excreted from the proventriculus. Since poultry do not have teeth, this section is required to break down the food and acts as a mechanical stomach. There are three parts to the small intestine, the duodenum, jejunum, and the ileum [42]. All three sections play a different role in absorbing nutrients and minerals, and pH in each section progressively increases towards neutrality, or a pH of 7.2 [43]. Two sacs, called ceca, are found at the end of the ileum, where the contents of the digestive tract are held until emptied through the cloaca [42]. Importantly, the microbial population is highest in the ileum and ceca, especially for *Lactobacillus* which can inhibit the colonization of pathogenic bacteria through the mechanisms discussed above [41].

2.2.4 Technical Challenges and Applications of Current Probiotic Formulations

As discussed in previous sections, probiotics may have many therapeutic applications in both humans and animals. Extensive research has been conducted on the ability of probiotics to prevent or treat illnesses such as diarrhea, respiratory infections, atopic dermatitis, and even cardiometabolic syndrome [44]. Probiotics may be effective in alleviating depression, showing how there may be a link between the gut microbiome and mental health, which would be a significant advancement in mental health research [45]. In the specific case of probiotic use in poultry studies have shown that they have many beneficial factors in addition to the antimicrobial activity inhibiting pathogens. Mohan et al. found that the addition of probiotics in feed improved the growth rate of broiler chickens [46], and Panda et al. showed that there was an increase in egg production from hens consuming feed that included probiotics [47]. Additionally, reports indicate that egg quality is also improved in laying hens upon consumption of probiotics, while egg

contamination is decreased [48]. Lastly, the shift away from antibiotics as growth promoters presents probiotics as an excellent alternative in agriculture. The evidence of the clinical efficacy of probiotics is continuously growing as more attention is dedicated to this field. This being said, concerns have also arisen regarding the quality and efficacy of current systems in both human and poultry applications [49].

Both conventional and non-conventional pharmaceutical systems have been developed for the delivery of probiotics; these include food-based products containing probiotics, which have been around for centuries, like yogurts, cheeses, and meats. Govender et al. described how the efficacy of probiotics using these food-based items is uncertain, as the viability of bacteria varies according to many factors, such as production and consumption of products [49]. The harsh conditions of the digestive system also impede the use of food-based probiotics, as they provide little to no protection once consumed. Significant time and money has been invested into pharmaceutical products to try to address the concerns faced by food-based probiotics and to make products more effective at delivering viable bacteria. Since probiotics aimed at enhancing the microflora are most effective when delivered to the intestine, commercial products are often made for oral delivery with probiotics encapsulated into tablets, capsules, or beads [49]. The cells are encapsulated into the core with a coating membrane surrounding the core, thus forming a barrier stabilizing and protecting the bacteria against the harsh conditions of the digestive system. There are three main types of encapsulation: reservoir, matrix, and coated matrix (Figure 4). For reservoir encapsulation, the substance is encapsulated into the core with a layer around it for coating. In a matrix, the encapsulated substance is dispersed within the coating material, and there is no designated location for an encapsulated core. Lastly, a coated matrix is a combination of the reservoir and matrix concepts, with a matrix-like encapsulation entirely covered by an additional

coating layer. The cells can be released according to a range of stimuli, such as pH change, heat, enzymatic activities, osmotic pressure etc. [50].

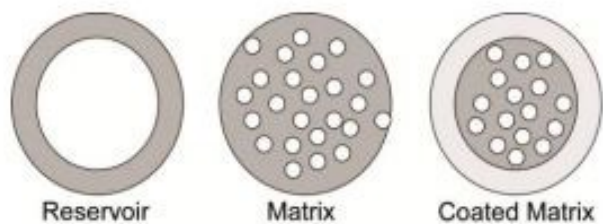


Figure 4. Three different ways for encapsulation of probiotics. Image from [50].

The material used to encapsulate the probiotics must be able to protect the cells during the production, storage and delivery stages. Polysaccharides, such as sodium alginate and chitosan, oligosaccharides – like sucrose and trehalose –and proteins, have all been used with differing encapsulation techniques [50]. Oligosaccharides are often used to preserve the cells as they prevent phase transitions of the cell membrane, which would otherwise affect the integrity of the membrane, resulting in leaks and damages to the cell [51]. This is further supported by multiple experimental reports showing the increase in cell viability with the addition of an oligosaccharide [52]. Furthermore, oligosaccharides are food-grade materials, making them safe for consumption. Methods to encapsulate probiotics include spray drying, lyophilization, extrusion, emulsion, and spray cooling [50]. These methodologies generally depend on the interactions between solutions or the use of external equipment to produce a bead/ droplet encapsulating the probiotics [53].

Health Canada follows the WHO definition of probiotics to be “live microorganisms that, when administered in adequate amounts, confer a health benefit to the host”. Furthermore, they have defined “adequate amounts” to be 10^9 colony forming units (CFU) per serving to be considered a probiotic product [54]. However, as we know, many cells are degraded due to the

manufacturing, processing, and storage steps, with both live and dead bacteria inevitably being delivered to the customer. Thus, in order to ensure that the advertised amount of viable bacteria is delivered at the time of consumption, capsules often contain higher doses. Not only are there concerns regarding the inefficiency of this methodology, there are also safety concerns with the consumption of large amounts of bacteria. The potency of the probiotics is especially concerning for individuals that are young or have immune disorders, as this may result in the imbalance of anti- and proinflammatory cytokines [55]. Some studies show that dead probiotic bacteria may still possess similar antimicrobial properties to live bacteria, but these concepts continue to be investigated. It has also been hypothesized that the wide range of responses to probiotics may be a result of the unknown variation in live and dead cells administered to the host [56]. Either way, pharmaceutical processes must be accurate and efficient when producing drugs, which is a significant concern with current processes.

2.3 Micromilling and micro-molding technologies

Microfabrication is a new and upcoming technology that utilizes engineering concepts to resolve limitations in various fields, including the pharmaceutical industry. Fox et al. have described how micro-particulate systems could address the many concerns associated with oral drug delivery, such as drug degradation, low drug solubility, and low drug permeability [57]. Microfabrication can be used to enhance current oral drug delivery methods by altering features at the microscale to improve the interaction between the drug system and the body. Of these features, geometry is likely one of the most important, as it allows for the utilization of the precise control in the design of the system for its application, such as a planar structure instead of the typical spherical particles. In comparison to a spherical particle, planar shaped particles increase the contact area for interaction with the epithelial lining, increasing drug permeation (Figure 5) [57].

Furthermore, planar particles decrease the force exerted on it by the intestinal fluid, further enhancing their adhesion to the epithelial lining. Lastly, the dissolution kinetics of the micro-fabricated system could be used for the co-delivery of multiple drugs to enhance viability and efficacy [57].

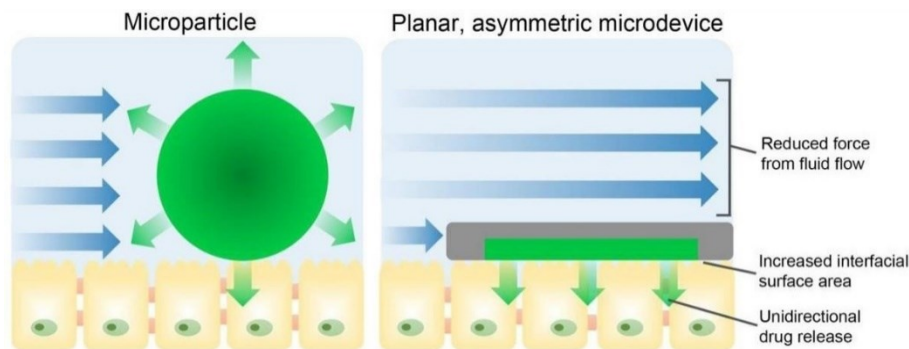


Figure 5. Comparison of spherical and planar microparticle for adhesion to epithelium lining. Image from [57].

Micromilling is a specific microfabrication process where a cutting tool is used to shape a metal into a desired design. Advancements in computer numerical control (CNC) have allowed for the automation of milling processes, and also improvements in the precision of the cutting tool [58]. Nowadays, micro-scale milling tools (as small as 10 μm in diameter [59]) can be used to produce micro-scale products for various medical applications, such as implantable medical devices and targeted drug delivery [60]. In the micromilling process, a three-dimensional design is created using a computer; it is then converted into a code that can be used by the micromilling machine. The coding determines the patterns taken by the milling bit to etch microstructures onto a metal plate or plastics [61].

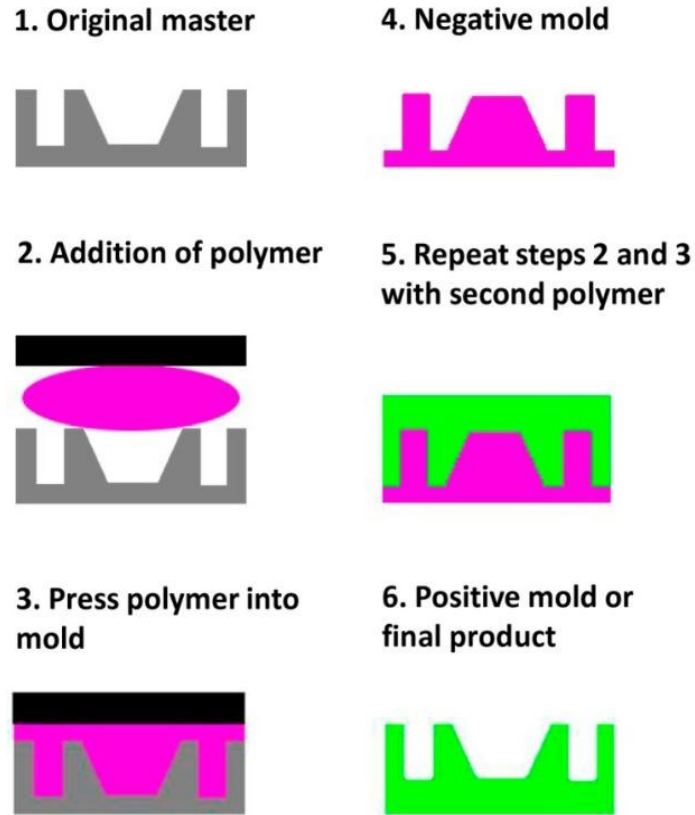


Figure 6. Fabrication steps for polymer molding. Image from [62].

A master mold is produced onto the micromilled metal plate, which can then be used in micro-molding technologies to replicate the mold with polymers such as polydimethylsiloxane (PDMS). An important aspect of PDMS is that it is a viscous liquid before curing, making it easy to work with and giving it the ability to replicate features at the nanometer scale for the creation of subsequent molds. A negative mold (polymer) is created from the original master mold (metal plate) by adding a thermoset polymer, such as PDMS, and allowing it to cure. As seen in Figure 6, the negative mold has the opposite design from the master, therefore it must be replicated with the polymer once again to produce a positive mold using, for example, polylactic acid (PLA) [62]. The PLA mold can then be used to fabricate PDMS molds used for casting microfabricated drugs.

Notably, micromilling enables the mass production and easy scale-up of micro fabricated technologies, as it is easy to replicate batches quickly and efficiently using the master mold [61].

3. Project design and hypotheses

The increasing awareness of the consequences associated with antibiotic-resistant bacteria has resulted in intentions to eliminate the use of antibiotics in agriculture in many countries including Canada. Specifically, significant efforts have been focused on developing alternate approaches to using antibiotics in removing antimicrobial agents in poultry. The use of probiotics in reducing the abundance of *Salmonella* in poultry presents an innovative opportunity for the development of a solid oral formulation that would significantly benefit the industry. A long-term stable, cold storage-free, efficient probiotic formulation would allow for significant cost reductions and a change in strategy for the entire agriculture industry.

Micromilling allows for the fabrication of conical frustum topographical features on aluminum master structures, followed by replication of the topographic structures on PLA/PDMS molds. The resulting PLA/PDMS mold provides a scaffold for producing probiotics easily through molding/demolding processes. Finally, the addition of a pH-sensitive polymer stabilizes the encapsulated therapeutic agents against the acidic pH of the stomach and releases them in the neutral/basic pH of the intestine.

The main hypothesis of this study is that the development of a highly effective, dose-sparing, and long-term stable probiotic formulation produced through a micromilling/molding process can significantly contribute to the prevention and control of pathogenic bacteria, such as *Salmonella*, in poultry farming.

3.1 Objectives

The first objective of this work was to fabricate conical architectures using a combination of micromilling and micro-molding technologies to encapsulate the probiotic bacterium *Lactobacillus acidophilus*. The second objective was to demonstrate the stability and efficacy of the resulting probiotic vector against harsh digestive conditions of poultry. Finally, short-term environmental stability tests were conducted to evaluate the stability of the formulation over time.

4. Materials and Methods

4.1 Aluminum master mold and PLA/PDMS casting mold fabrication

A micromilling machine (Microlution 363-S; Microlution Inc., Chicago, IL USA) equipped with a tungsten-carbide tip (Performance Micro Tool, Janesville, WI, USA) was used to fabricate an aluminum master mold. The end-mill tool had the following dimensions: 1.3 mm diameter, 40-44° helix angle, 2 flutes, 200-300 µm flute length, ø3.175 mm shank, 12.7 mm cutting length, and 38.1 mm total length. The structures were designed using Autodesk Fusion 360, and then optimized and validated. The G-code generated from the CAM software was used to control the tool path of the micromilling machine, as shown in Figure 7. A feed rate of 10 mm/min and a spindle speed of 20,000 rpm were used for the milling process. A heavy-duty coolant, EDM-30 (Rustlick Inc., DeWitt, IA, USA), was employed to reduce the amount of heat produced as a result of friction on the sample. Once the Al master mold was fabricated, a negative mold was produced using Dow SYLGARD 184 Silicone Encapsulant (PDMS) from Ellsworth Adhesives (Germantown, WI, USA). The vendor instructions were followed to produce the formulation, and all air bubbles were removed using a vacuum oven (SHEL LAB; Sheldon Manufacturing Inc., Cornelius, OR, USA). The degassed formulation was poured onto the surface of the aluminum mold, placed in a vacuum oven to remove any remaining air bubbles within the formulation, and

let to cure at 37 °C. This first generation PDMS mold was used to make a PLA mold by adding polylactic acid (PLA) pellets to the mold. The pellets were placed on the surface and melted in an oven at 200 °C. Air bubbles within the PLA were removed using the vacuum oven, cooled to room temperature (RT) to set, and then demolded. A second generation PDMS mold was produced from the PLA mold in a similar procedure as the first generation. This second generation PDMS mold was used for subsequent experiments.

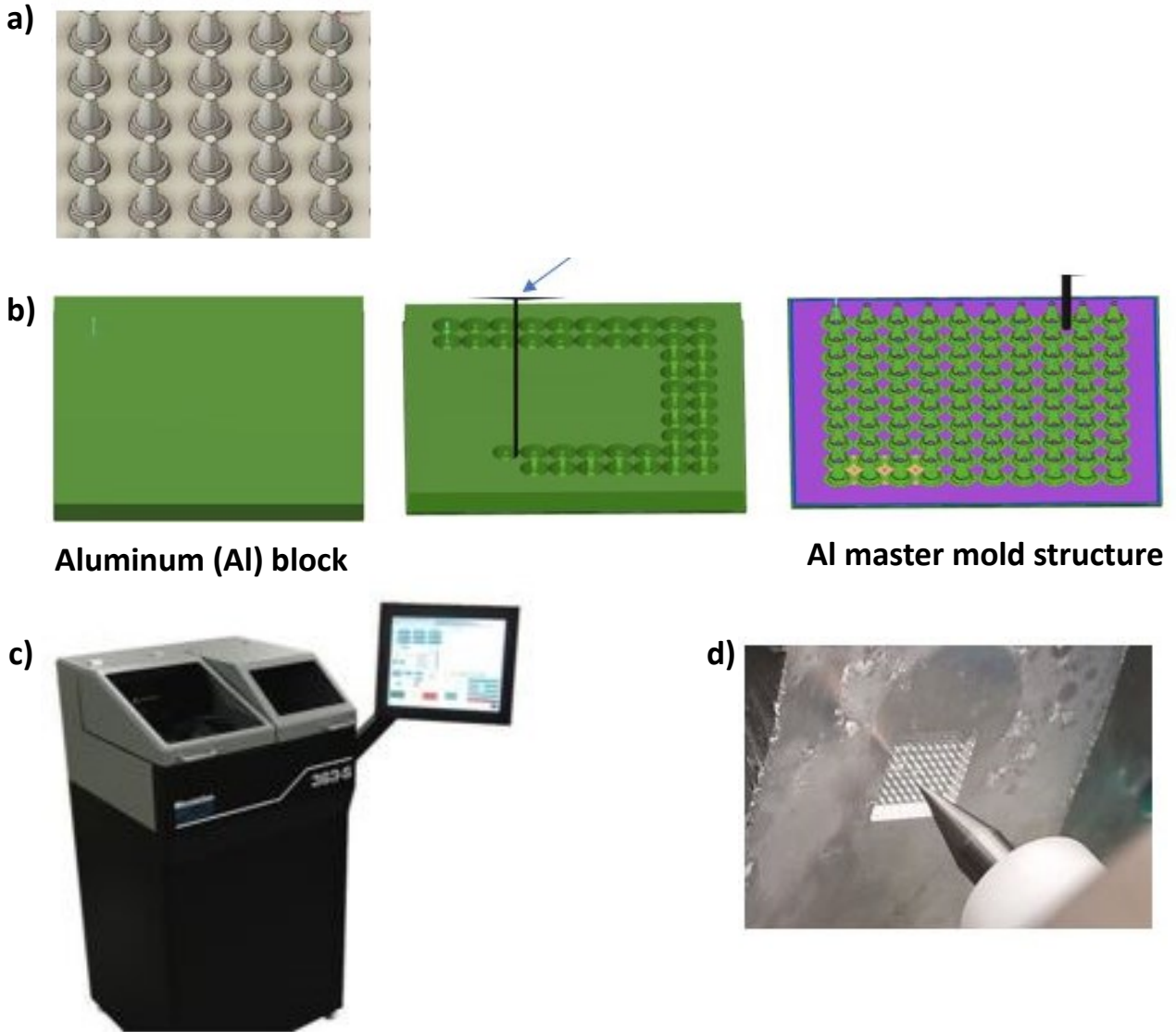


Figure 7. Fabrication with a micromilling machine. (a) Computer aided design, (b) simulation, (c) CNC machine, and (d) live image of fabrication.

4.2 Bacterial cell culture

Lactobacillus acidophilus (ATCC 4356) and *Salmonella typhimurium* (ATCC 14028) were obtained from Cedarlane (Burlington, Ontario, Canada) and propagated according to product sheet information. Media for *L. acidophilus* was prepared using MRS broth from Sigma-Aldrich (Cat# 69966; St. Louis, Missouri, USA) and following the vendor instructions. Nutrient broth (NB) from

Sigma-Aldrich (Cat# N7519) was prepared according to the vendor instructions and used to grow *S. typhimurium*. Agar plates were prepared in the same manner as the liquid broths with the addition of 1.5% agar powder flakes (Thermo Fisher Scientific, Cat # BP1423; Waltham, Massachusetts, USA). The optical density (OD) was measured at a wavelength of 595 nm using a plate reader (Bio Rad iMark Microplate Reader; Bio-Rad Laboratories, Inc., Hercules, California, USA). The data was read using a computer running the Microplate Manager Software (version 6.1). Since a 96-well plate was used to measure OD, pathlength correction was applied to normalize the OD for 200 μ L.

Cell stocks were prepared of both *L. acidophilus* and *S. typhimurium* by inoculating a single colony from propagation into 3 mL of broth and incubating overnight at 37 °C. 1 mL of the overnight culture was added to 500 mL of fresh broth in a 1-L flask, and incubated according to growth conditions. Once the growth reached OD₅₉₅ ~0.8, 800 μ L of culture were added to 200 μ L of 30% sterile glycerol solution in a cryogenic vial. Vials were stored in a -80 °C freezer until use.

Cultures of *L. acidophilus* were grown by adding 2.4 mL of cell stock thawed at RT to a sterile 500-mL flask containing 300 mL of fresh MRS broth. The culture was incubated in a CO₂ incubator (3100, Thermo Fisher Scientific) at 37 °C and 5% CO₂. Cultures were incubated until stationary phase was reached, as determined by a growth curve. For *S. typhimurium*, liquid cultures were grown by inoculating 100 μ L of cell stock into 10 mL of fresh NB, and incubated at 37 °C and 200 rpm.

4.3 Fabrication of probiotics patch

Low viscosity carboxymethylcellulose (CMC) sodium salt (Cat #C5678), sucrose (Cat #84097), trehalose dihydrate (Cat# 90210), and sulforhodamine B (abbreviated as SB dye

hereafter; Cat #230162) were obtained from Sigma-Aldrich. Phosphate Buffered Saline (PBS), 10× solution from Fisher Scientific (Cat# BP3994) was used to make 1×PBS by diluting the PBS with DI water in a ratio of 1:9.

A process flow for the fabrication of the probiotic patch is represented in Figure 8. Upon fabrication of the PDMS molds by micromilling and mold casting, *L. acidophilus* cells or SB dye were encapsulated using established procedures adapted for biological samples. *L. acidophilus* cells were collected at the stationary phase and washed by centrifugation (Eppendorf 5804) three times with PBS and one time with DI water for 10 min at $13,416 \times g$ and 4 °C. The pellets were suspended in 200 μL of DI water, combined, and labelled as “cells”. The probiotic formulation used in this work was composed of 1:1:2 ratio of cells: DI: 15 wt% trehalose + 0.5 wt% CMC. For SB dye, the formulation consisted of a 2 v/v% concentration of SB dye with 15 wt% trehalose + 0.5 wt% CMC. Approximately 250 μL of the formulation was added to the surface of the mold and spread using a pipette tip. A vacuum oven was then used to run 6 cycles to remove any air bubbles in the encapsulation solution. Any excess solution was removed from the top surface of the mold and discarded. A 50-mL falcon tube filled with approximately 45 mL of cured PDMS provided a flat surface for the molds during centrifugation. They were centrifuged for 5 min at $1,207 \times g$ and 24 °C to ensure the encapsulation solution was captured into the conical structures of the molds, and any excess solution was removed using filter paper. The molds were then dried in an incubator at 37 °C for 4 h. A CMC backing formulated of 15 wt% low viscosity CMC + 10 wt% sucrose was added and spread across the mold evenly through a horizontal motion only. The molds were once again placed in a vacuum oven for 4 cycles (to remove any air bubbles in the CMC backing) and incubated overnight at 37 °C. Finally, the structures were carefully demolded from the PDMS mold manually.

4.4 Spray coating

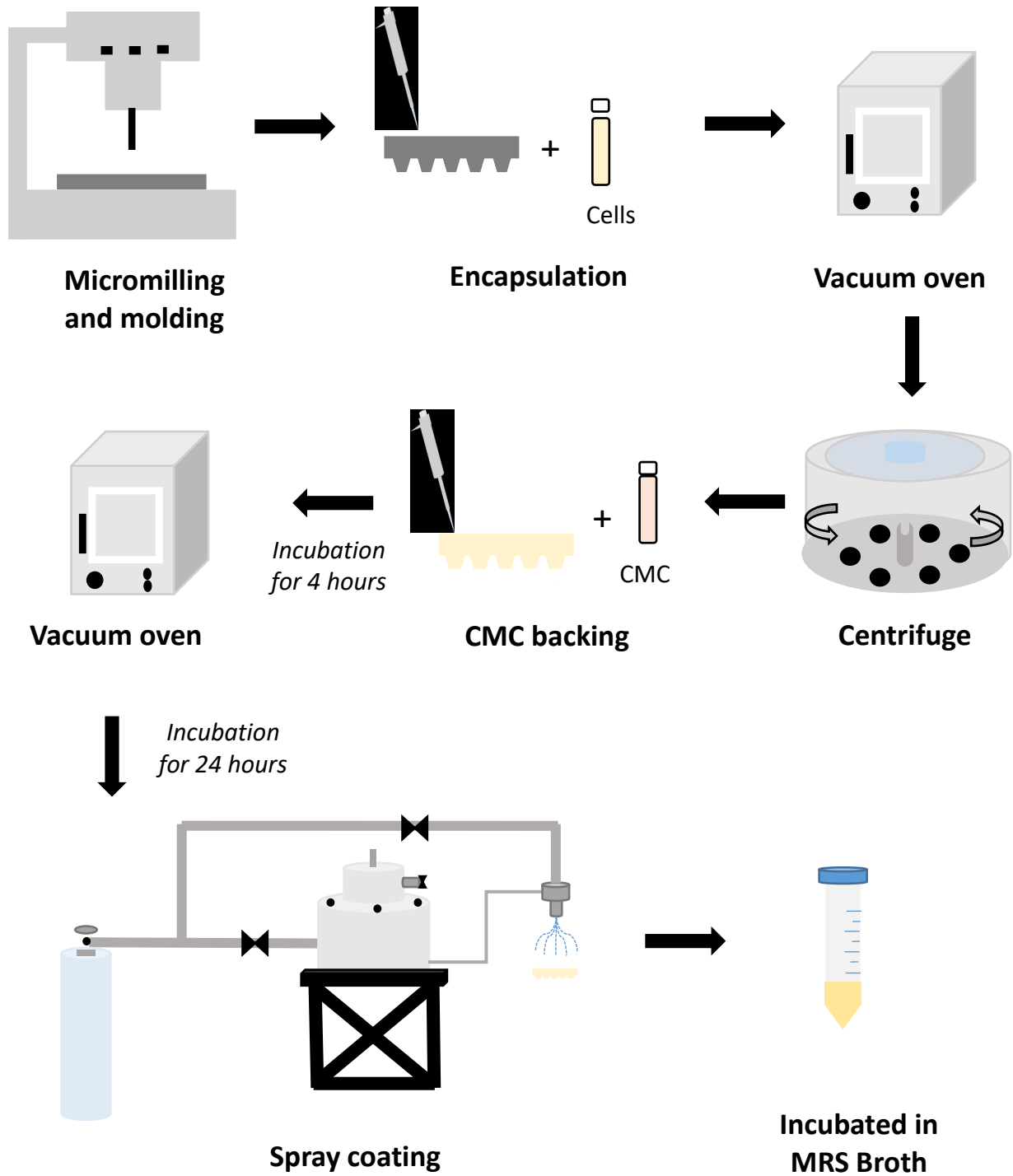


Figure 8. Schematic representation of the probiotic patch fabrication process.

EUDRAGIT® S 100 polymer (abbreviated as S100) was received from Evonik Canada Industries (Burlington, Ontario, Canada). Methylene chloride (DCM; Cat # D37-4), isopropanol (Cat #BP26181), and reagent alcohol (Ethanol) (Cat # A962P-4) were obtained from Fisher Scientific. A co-solvent, consisting of DCM: isopropanol: ethanol in a 2:1:1 v/v ratio, was used to prepare 5 wt% stock solution by dissolving Eudragit S 100. As seen in Figure 9, the solution vessel was attached to a nitrogen (N₂) gas line in order to pressurize it, and another N₂ gas line was connected to the spray nozzle. Various parameters – such as pressure, platform distance, and spray coating time – were tested to optimize the coating conditions. The final procedure was to keep the N₂ gas cylinder set to 60 psi and the platform distance to 23 cm from the spray nozzle. The microstructures were analyzed using scanning electron microscope (SEM). Micrographs were obtained using a Hitachi S-3000 (Mississauga, Ontario, Canada) operating at 15 kV, 80 μA, with a working distance of 15 cm and running a PC-SEM software. The samples were dried at 40 °C for 24 h prior to analysis, and cut into 1x1 cm² squares. Carbon tape was used to hold samples during analysis. These were coated with 10 nm gold using a multi-cathode sputter deposition (Denton Vacuum Inc., Moorestown, NJ, USA) operating at 1 mTorr. The back (flat) side of the patches were coated first, allowed to dry in an incubator at 37 °C for 3 h, then the conical structures were spray coated, followed by drying at 37 °C overnight. A Q-tip was used to ensure sufficient coating of the edges of the probiotic patch with the polymer solution. The patches were placed to dry for an additional 3 h in an incubator at 37 °C.

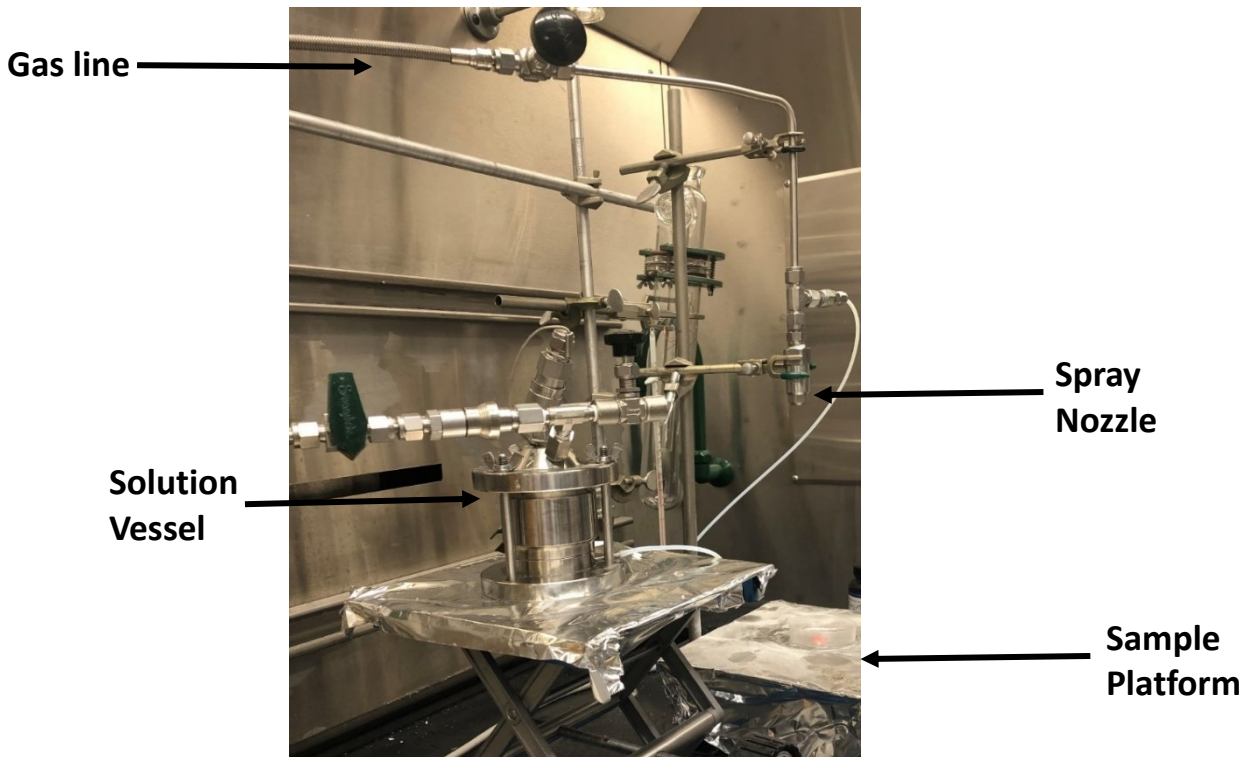


Figure 9. Spray coating process set up.

4.5 Characterization of cell viability during fabrication process

The effects of the vacuum oven, centrifugation, incubation time, and the CMC backing on cell viability were evaluated at various fabrication steps by immersing a PDMS mold with encapsulated probiotic formulation into a well of a 6-well plate. Each well contained 1 mL of DI, and the PDMS molds were placed face down into the DI and soaked for 1 h at RT on a platform shaker (VWR, Radnor, Pennsylvania, USA) at a speed of 4. The PDMS mold was removed using a tweezer and rinsed with DI to ensure all of the encapsulated formulation was removed from PDMS molds. Similarly, demolded samples (with a CMC backing) were placed with the conical structures downwards and fully dissolved in a well with 1 mL of DI after 90 s. The remaining solution in the well was added to a 2-mL Eppendorf tube and centrifuge-washed twice with DI water for 5 min at $17,005 \times g$ and $4 \text{ }^\circ\text{C}$. During the final wash, all excess solution was removed from the walls of the tube using Kimwipes, and the pellet was suspended in DI to a final volume

of 1.0 mL. For measurements with the demolded samples, this final 1.0 mL solution (containing the pellet and DI) were added to a 50-mL Flacon tube containing 4 mL of MRS broth at RT, and incubated according to growth conditions.

To determine the formulation effect, the encapsulation formulation (from encapsulation procedures) was poured into a 50-mL Falcon tube (cells: DI: 15 wt% trehalose + 0.5 wt% CMC in a ratio of 1:1:2). Another 50-mL Falcon tube containing a ratio of cells: DI of 1:3 was used for comparison. These tubes were placed on an automatic rotator at RT for 24 h and the protein concentration and cell count of the suspensions were measured periodically.

4.6 Stability in simulated digestive conditions

Pepsin from porcine gastric mucosa (Cat #P7000), pancreatin from porcine pancreas (Cat #P7545), and potassium chloride (KCl; Cat #P9333) were obtained from Sigma-Aldrich. Hydrochloric acid (HCl; Cat # A144S) and sodium phosphate dibasic anhydrous (Na_2HPO_4) (Cat # S374-1) were obtained from Fisher scientific. pH of the solutions was measured using a pH meter (Hanna Instruments, Woonsocket, Rhode Island, USA) calibrated according to vendor instructions prior to use. Simulated gastric and intestinal solutions for *in vitro* digestive procedures were modified from Sommerfeld et al. [63]. Two samples were added into 50-mL Falcon tubes with the corresponding solutions (i.e., gastric or intestinal fluids). The simulated gastric fluid (SGF) consisted of 0.2M KCl, 0.2M HCl (added dropwise to obtain a pH of 2.0) and 3,000 U of pepsin. A 50-mL Falcon tube containing 5 mL total of the gastric fluid was incubated in a water bath (Walter Products Inc.) set at a temperature of 40 °C for 45 min. Then, 0.1 wt% Na_2HPO_4 solution was added dropwise to the SGF with 3.7 mg/mL of pancreatin to reach a pH of 7.1 to create the simulated intestinal fluid (SIF). This SIF was incubated in the water bath for an additional 60 min.

Upon completion of the incubation for biological samples (i.e., *L. acidophilus*), the solution was centrifuged for 5 min at $13,416 \times g$ and $4\text{ }^{\circ}\text{C}$ to remove the buffer and enzymes. Subsequent to the addition of MRS at RT, the samples were incubated according to growth conditions.

4.6.1 Dye release tests:

For SB dye release tests, the same *in vitro* digestive procedures were followed as above. Samples encapsulated with SB dye were exposed to the simulated gastric conditions followed by the intestinal conditions. 100 μL of the sample were pipetted into a 96-well plate every 10 min. Fluorescence was measured using a microplate reader (Cytation5; BioTek, Winooski, Vermont, USA). The data was read using a computer running Gen5 Software (version 2.09). A fluorescence spectrum was measured using an excitation of 540 nm and emission range of 560 to 620 nm with 1 nm steps.

4.6.2 Environmental stability test:

Probiotic samples with a protection layer (spray coated) were exposed to harsh environmental storage conditions to characterize the protective efficacy of the protection layer made of S100 polymer. The stability of the samples was measured at the conditions listed in Table 1. The samples were incubated at $37\text{ }^{\circ}\text{C}$ and 70% relative humidity (RH) for either 1 day or 1 week in an environmental chamber (HPP260; Memmert, Schwabach, Germany). For comparison purposes, probiotic patches were stored in sealed and unsealed containers and their time-dependent stability change was monitored at day 1 and week 1 post-storage. To prepare sealed storage samples, 60-mL bottles containing probiotic patches were flushed with N_2 gas, followed by sealing

using an electromagnetic induction sealer (CapsulCN). Stability of the probiotic patches were measured following the same procedure addressed above in a simulated digestive condition.

Table 1. Stability test conditions

Time	Condition		
	Storage	Sample	Testing
1 day	Sealed	Spray coated	Digestive
		Bare	DI
	Unsealed	Spray coated	Digestive
		Bare	DI
1 week	Sealed	Spray coated	Digestive
		Bare	DI
	Unsealed	Spray coated	Digestive
		Bare	DI

4.7 Characterization

4.7.1 Colony Forming Units (CFU)

Drop plate CFU was used to measure the number of viable cells. The method was adapted from Naghili et al., where 2 μ L from the sample were spotted onto the agar plate using a pipetter and allowed to absorb fully [64]. 10-fold dilutions were made using DI water and all measurements were performed in triplicates. Agar plates were then incubated in a CO₂ incubator at 37 °C and 5% CO₂ for 48 h.

4.7.2 Agar well diffusion test

The antimicrobial activity of the patches was evaluated using the agar well diffusion method adapted and modified from Shokryazdan et al. [65]. A well was punctured into an MRS agar plate using the base of a 1-mL pipette tip. 100 μ L of the *L. acidophilus* sample were added to

the well and allowed to diffuse into the agar by incubating at 37 °C and 5% CO₂ overnight. A soft NB agar overlay was made using the vendor instructions for liquid NB with the addition of 0.5% agar powder flakes. Then, 10⁸ CFU/mL of *S. typhimurium* were added to 30 mL of the soft NB agar overlay. The soft NB agar overlay was then spread around the wells and incubated overnight at 37 °C and 5% CO₂. The inhibition zone diameter was then measured. All measurements were performed in triplicates.

4.7.3 Protein concentration

Micro BCA Protein Assay Kit (Cat #23235) from Thermo Fisher Scientific was used. Vendor protocols were followed to quantify the protein concentrations of samples and all dilutions were made using DI water. A 0 – 200 µg/mL bovine serum albumin (BSA) standard curve was prepared and measured each time. 100 µL of working reagent were added to 100 µL of sample in a 96-well plate and mixed by pipetting up and down. The plate was covered with aluminum foil and incubated at 45 °C for 45 min. Absorbance at a wavelength of 560 nm was then measured using a plate reader (Bio Rad iMark Microplate Reader). The data was read using a computer running the Bio-Rad Microplate Manager Software (version 6.1) with a 4-parameter fit. All samples were measured in triplicate and at least 3 dilutions were used to quantify the protein concentration.

4.7.4 Optical microscopy

A stereomicroscope (Cole-Parmer, Montreal, Quebec, Canada) with a haloid lamp (AmScope, Los Angeles, California, USA) was used for microscopy analysis. Images were

captured with a computer using a Moticam (Motic, Richmond, British Columbia, Canada) 2.0MP digital camera operating Motic Image Plus software (version 3.0).

4.8 Statistical analysis

Standard deviations were calculated using the built-in tool in excel. For results of CFU/protein concentration, the division arithmetic calculations for error propagation were used. PSPP (developed by GNU) was used to conduct analysis of variance (ANOVA) with Tukey test set at a 95% confidence interval.

5. Results and Discussion

5.1 Mold Fabrication

Figure 10a and 10b show optical microscopy images of the 10×10 array of conical structures on an aluminum master mold produced from the micromilling machine. Due to the number of line and arc commands in the G-code, the surface of the conical structures in the aluminum mold was found to exhibit unwanted machining debris and a rough surface finish during the first micromilling process (Figure 10a). This debris would cause issues fabricating subsequent PDMS molds with fine engraved architecture. Thus, a smoothing G-code was created with higher feed rates, new path parameters, and tight tolerance positions to remove these marks after fabrication. As seen in Figure 10b, the secondary micromilling process was proven to be effective in smoothing the surface. Furthermore, SEM analysis was performed on the negative PDMS mold fabricated from the smoothed aluminum master mold. As seen in Figure 10c, consistent structures with no irregularities were observed on the surface or within the conical structures. Additionally,

the PDMS accurately replicated structures even at the micro scale, as shown by the successful replication of the fine grooves at the base of the conical structures.

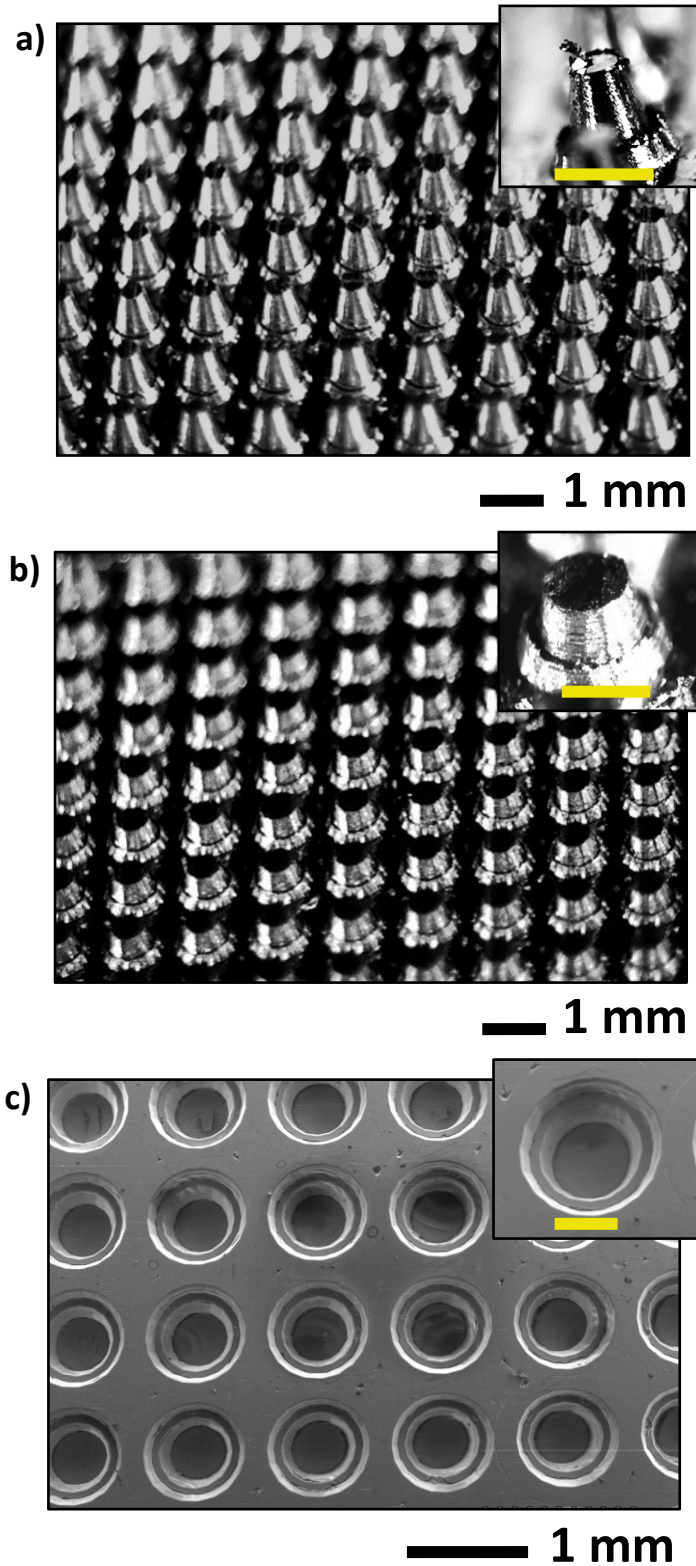


Figure 10. Aluminum master structure. (a) Before smoothing, (b) after smoothing, and (c) SEM image of a negative PDMS mold from the aluminum master structure after smoothing. Inset image represents a high magnification image where scale bar is 500 μm .

5.2 Effect of Fabrication Process on Cell Viability

The protective abilities of trehalose on *L. acidophilus* cells are shown in Figure 11a. At RT, the addition of 15 wt% trehalose + 0.5 wt% CMC to a formulation consisting of DI and *L. acidophilus* cells resulted in a higher cell viability than a formulation made of just DI. The time period tested correlated to significant points in the fabrication process, where Time 0 was defined as when the basic encapsulation procedures are completed (once all air bubbles and excess formulation are removed). Similarly, Time 4 indicates the point after a 4 h-incubation, corresponding to when the CMC backing would normally be added. Finally, Time 24 indicates the time point after incubation of the molds for 24 h, equivalent to the time when the molds are demolded, before spray coating. It should be noted that the viability in Figure 11a was measured using only the formulation suspension, and not by encapsulating the formulation in PDMS molds. Although there was a decrease in cell viability over time for all samples, higher levels of cell viability were consistently observed with the addition of trehalose. This improvement in cell viability is consistent with the stabilizing effect of trehalose observed for biomolecules, as expected according to literature; hence trehalose was used for the remainder of experiments [51].

To determine the effect of vacuum encapsulation, centrifugation, and incubation time on the cell viability, cells formulated with trehalose were encapsulated in PDMS molds and tested after various time periods of incubation at 37 °C. All samples encapsulated originated from the same batch to ensure no formulation or process differences would interfere with the results. Samples were separated into 3 groups to test at the significant points in the encapsulation process (Times 0, 4, and 24 h). As seen in Figure 11b, the incubation time in the encapsulation process had no significant effect on the cell viability over the course of incubation up to 24 h. These findings support the conclusion that the *L. acidophilus* cells were successfully encapsulated into the PDMS

molds and that the initial encapsulation procedures and incubation time period had no effect on cell viability. Interestingly, there is a decrease in cell viability over time for the cells suspended in trehalose (Figure 11a), but the same trend is not evident for cells encapsulated in the PDMS molds (Figure 11b). This difference is likely attributed to the incubation temperatures used, as the cells suspended in the trehalose formulation (in Figure 11a) were incubated at RT and those encapsulated in the PDMS molds (in Figure 11b) were incubated at 37 °C. Thus, 37 °C was used as the incubation temperature for the remainder of experiments.

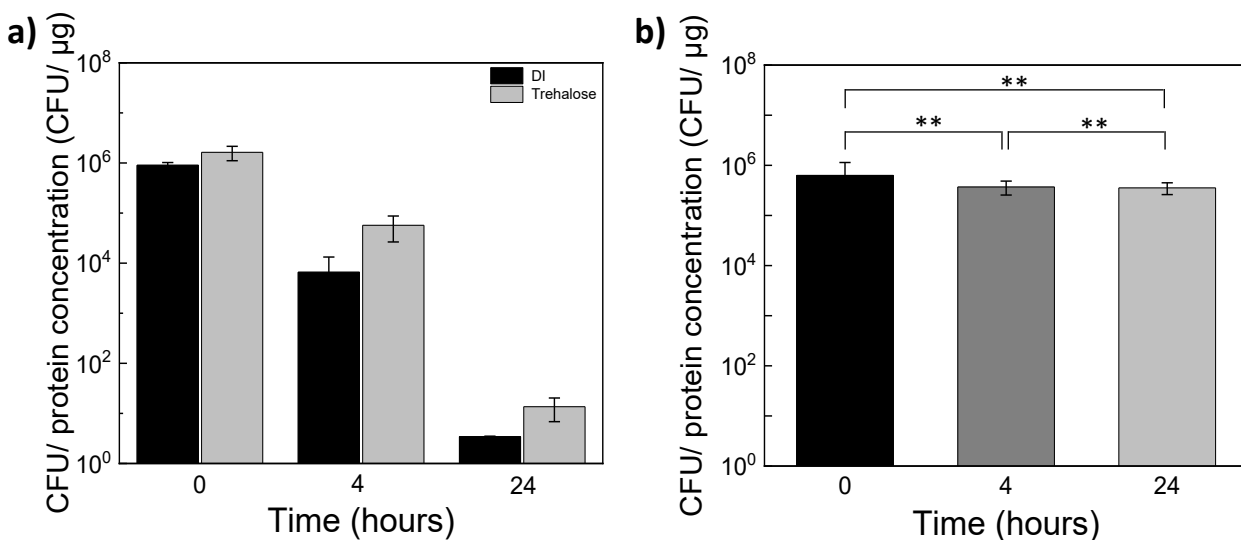


Figure 11. *L. acidophilus* cell viability. (a) Cell stability in a suspension of DI and trehalose for various incubation periods at RT, and (b) the effect of corresponding process incubation periods at 37 °C on cells encapsulated in a PDMS mold. The mean value was calculated from 3 replicates and the error bars indicate standard deviation. Note: ** p-value > 0.05 by ANOVA.

Figure 12 shows the process flow diagram for the fabrication of *L. acidophilus* encapsulated probiotic patch formulation. Samples at two different parts of the fabrication process were collected to investigate the effect of the addition of the CMC backing on the measurement of *L. acidophilus* cell viability. “**Molded w/o backing**” represents the probiotic patch after the 4-h drying

process without a CMC backing, and “**Demolded w/ backing**” is after 24 h of drying with the addition of the CMC backing.

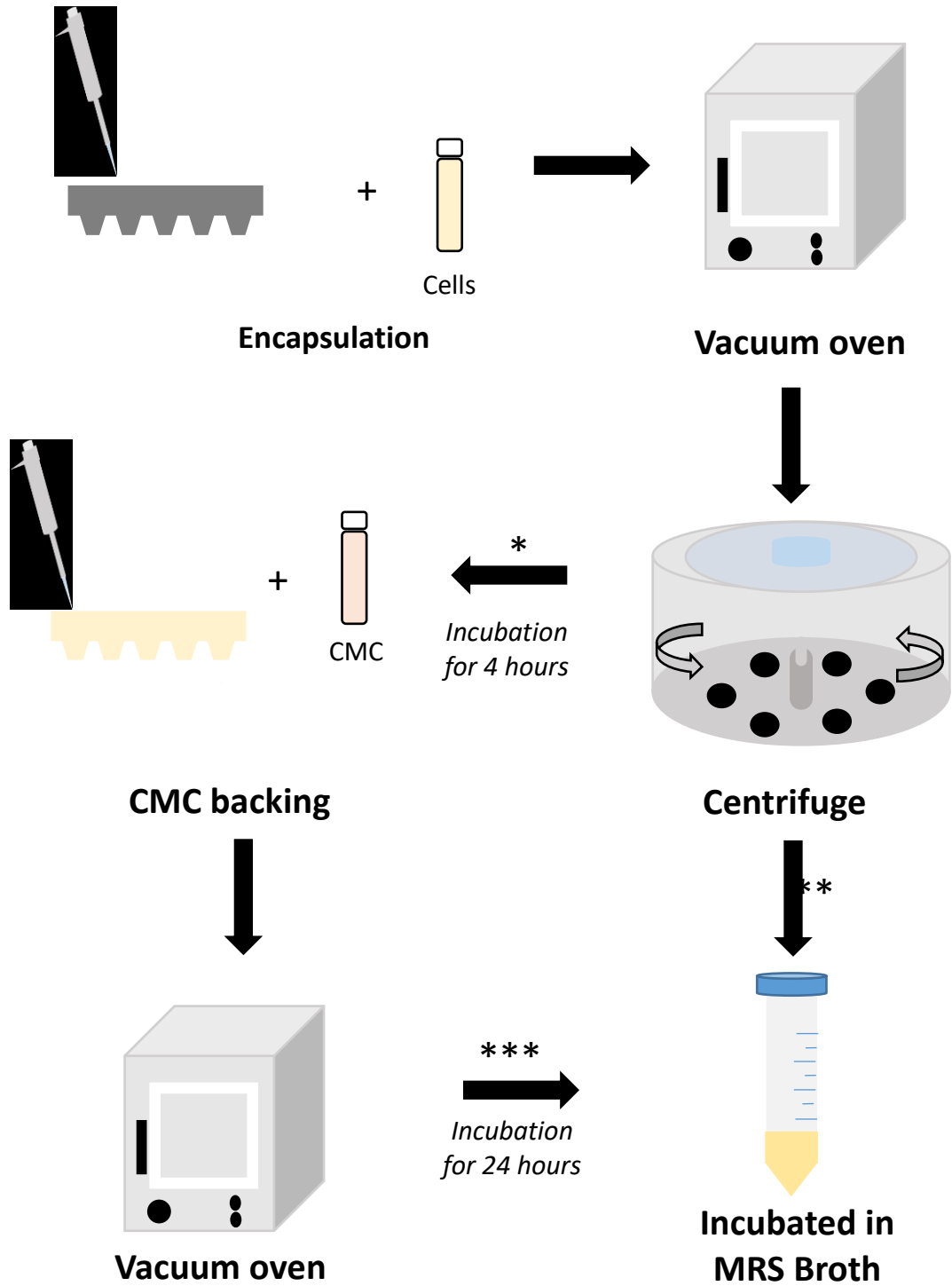


Figure 12. Schematic representation of the probiotic patch fabrication process. Note: * **Molded w/o backing**, ** **Molded w/o backing MRS**, *** **Demolded w/ backing MRS**.

As shown in Figure 13a and b, no significant cell viability was measured for demolded samples with CMC backing when incubated in MRS broth for 6 and 12 hours. However, incubation of **Demolded** w/ backing MRS samples in MRS for 24 h exhibited a significant increase in CFU values (Figure 13c), followed by a similar level of CFU in comparison to **Molded** w/o backing MRS samples after 48 h of incubation in MRS (Figure 13d). This marked increase in CFU might be associated with the encapsulated cells being in a dormant stage while in the solid trehalose formulation as they adapt to their new environment (i.e., liquid-to-solid state and solid-to-liquid state). That is, the probiotic cells may enter a dormant stage to protect themselves from various environmental stresses, such as dehydration during the processing steps. During this time, the cells in the solid formulation may have low metabolic activity [66], [67]. However, upon exposure to a more hospitable environment, such as incubation in MRS broth at 37 °C, they may regain their ability to replicate after adaptation to this new environment [68]. Longer adaption of the cells in the solid state to the changing environment explains why **Demolded** w/ backing MRS samples showed a rapid increase in their CFU values with the increase of incubation time in MRS broth (particularly after 12 h). As such, the cells in the patch formulation likely become culturable (incubation for around 24 h) and are assumed to exit the dormant stage and regain viability after incubation for approximately 48 h in MRS.

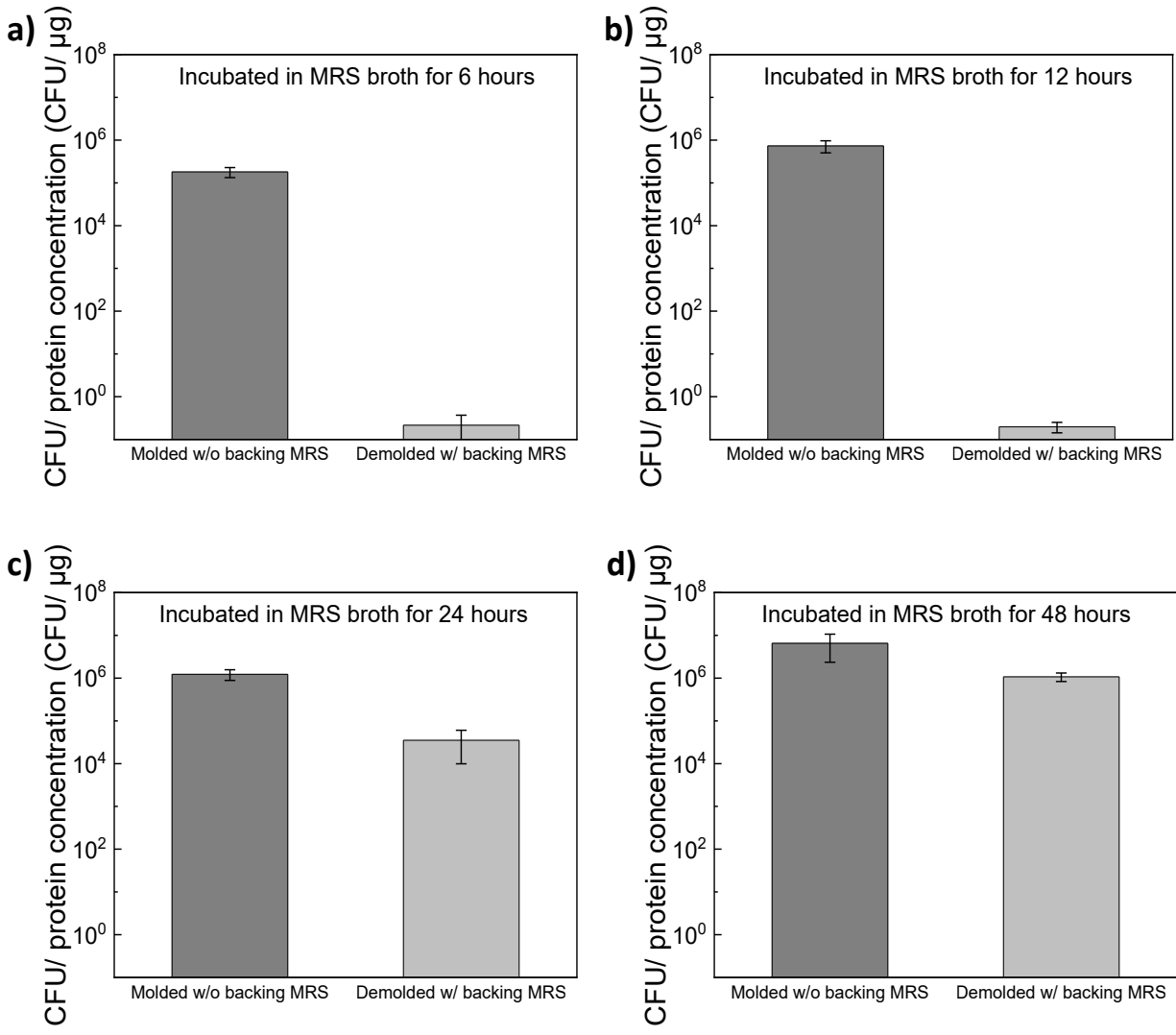


Figure 13. Change in cell viability of samples, i) molded without a CMC backing and ii) demolded with a CMC backing, with the increase of incubation time in MRS broth ((a) 6 hours, (b) 12 hours, (c) 24 hours, and (d) 48 hours). The mean value was calculated from 3 replicates and the error bars indicate standard deviation.

To better understand the lag in cell growth from samples **Demolded** w/ backing due to the cells being in a dormant stage, three batches of experiments were independently conducted to confirm the effect of incubation time in MRS broth on cell viability. To this end, the CFU values of samples **Molded** w/o backing measured directly after dissolving in DI were compared with those measured from **Molded** w/o backing MRS and **Demolded** w/ backing MRS samples, which were incubated in MRS broth for 48 h and then measured. As shown in Figure 14, it is evident that samples **Molded** w/o backing MRS displayed a significant increase in viability compared to **Molded** w/o backing that were not incubated in MRS broth. Also, as observed in Figure 13, a similarly high level of cell viability was seen from **Demolded** w/ backing MRS patch samples compared to **Molded** w/o backing MRS. It can be concluded that incubating the samples in MRS broth does not only provide a hospitable environment for cells to reactivate from the dormant stage, but also likely contributes to the growth of cells after 48 h of incubation. Therefore, **Molded** w/o backing MRS and **Demolded** w/ backing MRS sample measurements did not correlate to the exact same amount of initial cells encapsulated, but the incubation in MRS broth was assumed to be required to reactivate the cells from their dormant state.

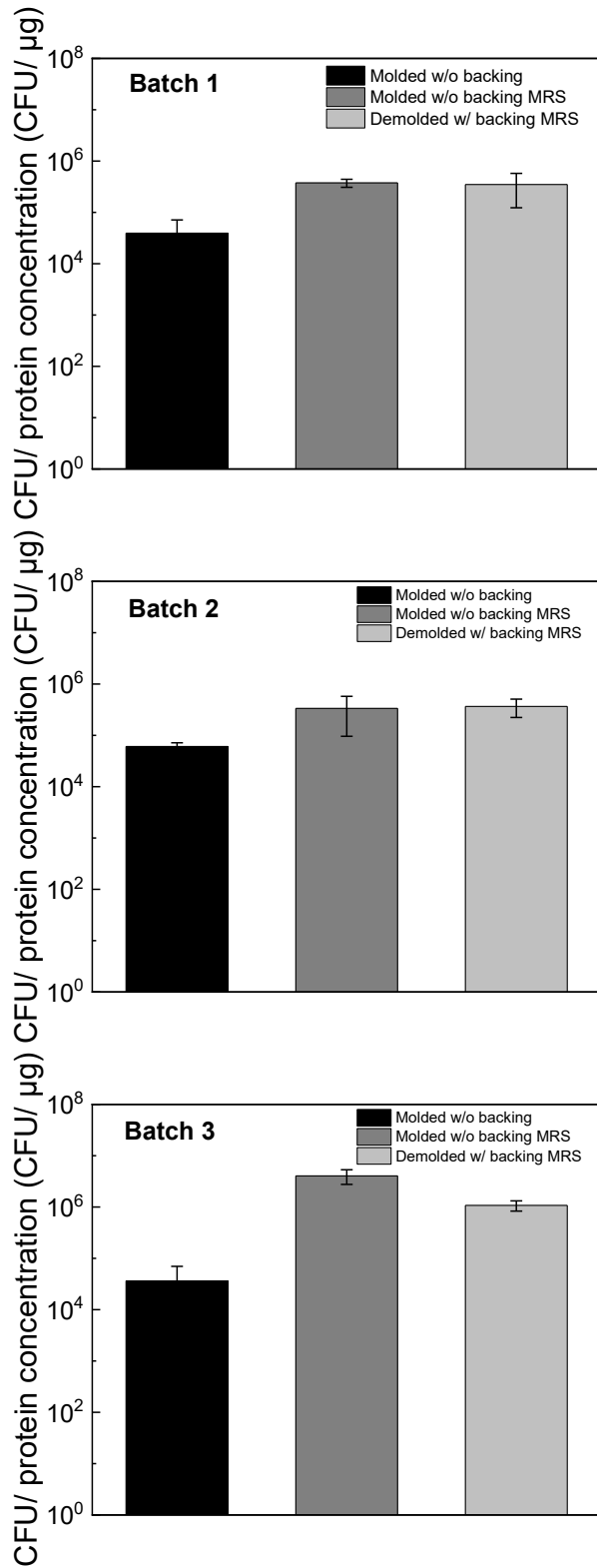


Figure 14. Cell viability of samples incubated in MRS broth for 48 hours i) molded without a CMC backing, and ii) demolded with a CMC backing in comparison to iii) molded without a CMC backing and directly measured without incubation in MRS broth. The mean value was calculated from 3 replicates and the error bars indicate standard deviation.

5.3 SB Dye Release Test

The release behavior of the encapsulated agent of the demolded samples was investigated by using SB dye as a model drug. It is important to determine if the conical structures of the demolded probiotic patch would dissolve to ensure that the cells encapsulated would be fully released in aqueous solution. Figure 15 shows the fluorescence microscopy images of SB dye-encapsulated patch with a CMC backing before and after exposure to DI water (Figure 15). The homogeneous distribution of SB dye seen in Figure 15a indicates that SB dye was successfully encapsulated into the conical structures of the mold by employing our patch fabrication process, and that the CMC backing provides sufficient support to keep the structures intact when demolding the patch. As shown in Figure 15b, it is evident that upon exposure to DI water, the conical structures began to dissolve and completely released the encapsulated model drug after 90 s. Moreover, the majority of the dye was released, as only minimal amounts remained on the base of the CMC backing after exposure to DI. The slight amounts of SB visible on the background could be attributed to SB being diffused into the CMC backing during the fabrication process. This means that the majority of *L. acidophilus* cells (which are significantly larger than SB dye molecules) encapsulated in our patch formulation would not interact with the CMC backing. Importantly, the CMC backing did dissolve, albeit at a slower rate, but the dissolution rate was not quantified.

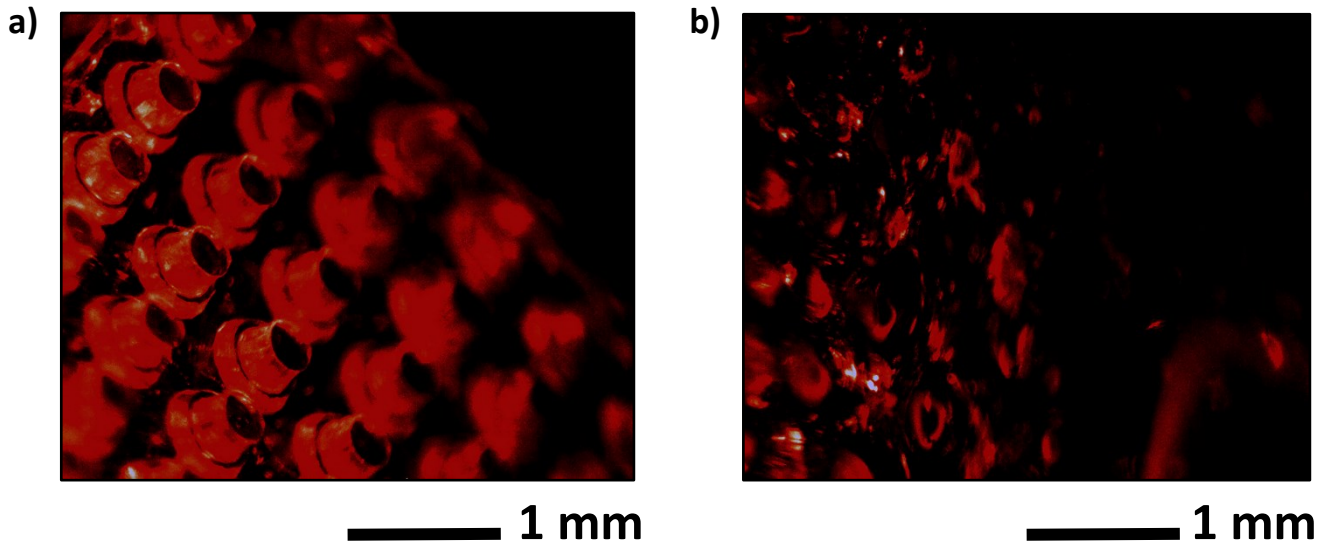


Figure 15. Fluorescent images of SB dye encapsulated molds release behavior. (a) Before and (b) after exposure to DI for 90 seconds.

5.4 Formation of a Protection Layer via Spray Coating of S100 Anionic Copolymers

In order to improve the coating conditions for the formation of a passivation layer on the patch, we first monitored the time-dependent S100 polymer coating thickness using the spraying coating setup shown in Figure 9. The thickness of the polymer coating on a silicon wafer was measured from SEM images analyzed at three different coating times (2, 5, and 10 s). As seen in Figure 16 it is evident that the thickness of the passivation layer increased with coating time (see Table 2 for thickness measurements). As shown in Figure 17, a linear relationship can be seen upon plotting the protection layer thickness against the corresponding spray coating time. From the linear curve fitting, the coating rate was found to be $1.076 \mu\text{m}/\text{sec}$ under our experimental conditions.

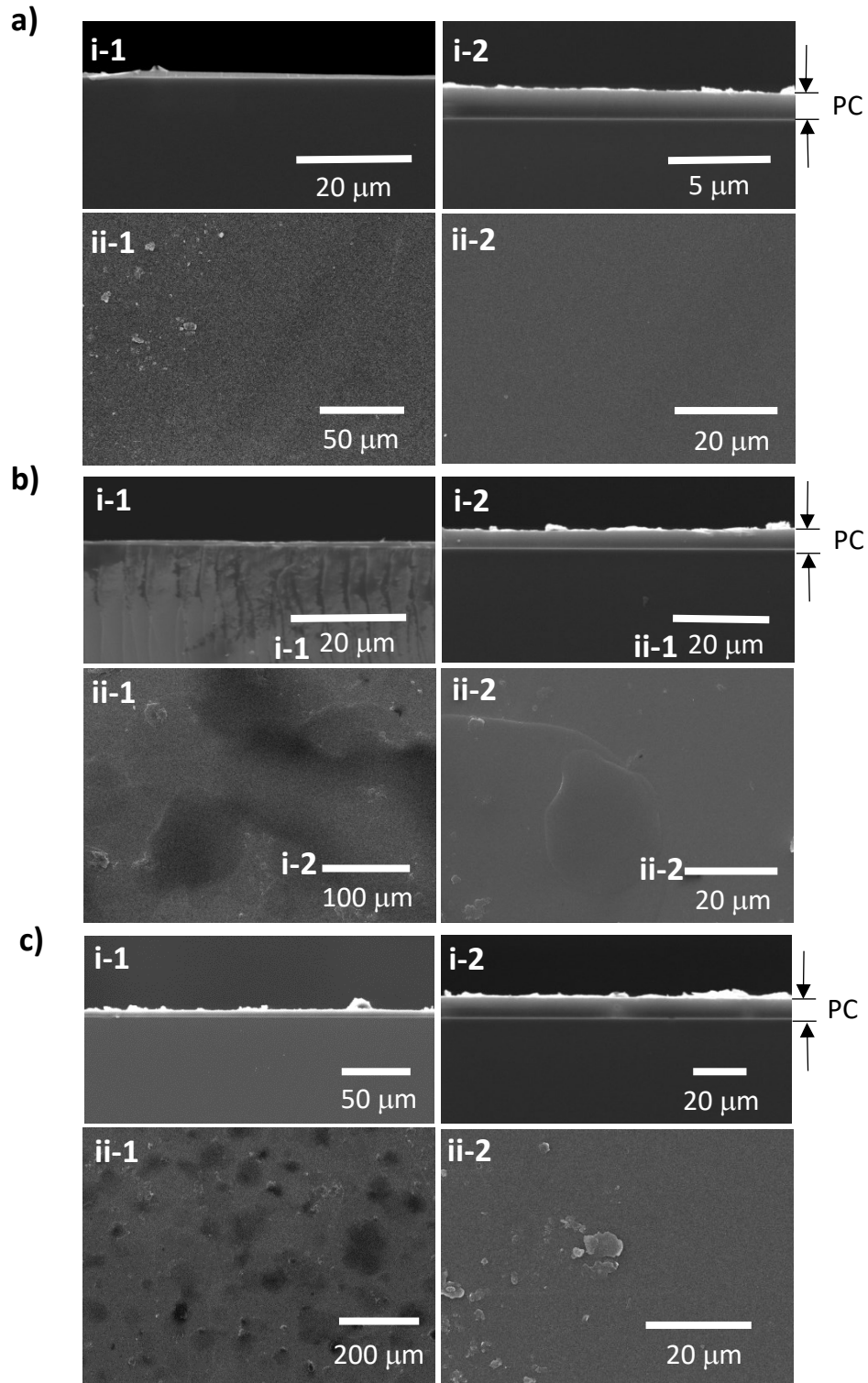


Figure 16. SEM images of a spray coated silicon wafer after (a) 2 seconds of coating, (b) 5 seconds of coating, and (c) 10 seconds of coating (i: cross-sectional view, ii: top view). Note: PC is polymer coating on top of the silicon wafer.

Table 2. Protection layer thickness according to SEM image analysis

Spray coating time (seconds)	Coating thickness (μm)
2	1.89 ± 0.90
5	4.60 ± 1.30
10	11.2 ± 2.4

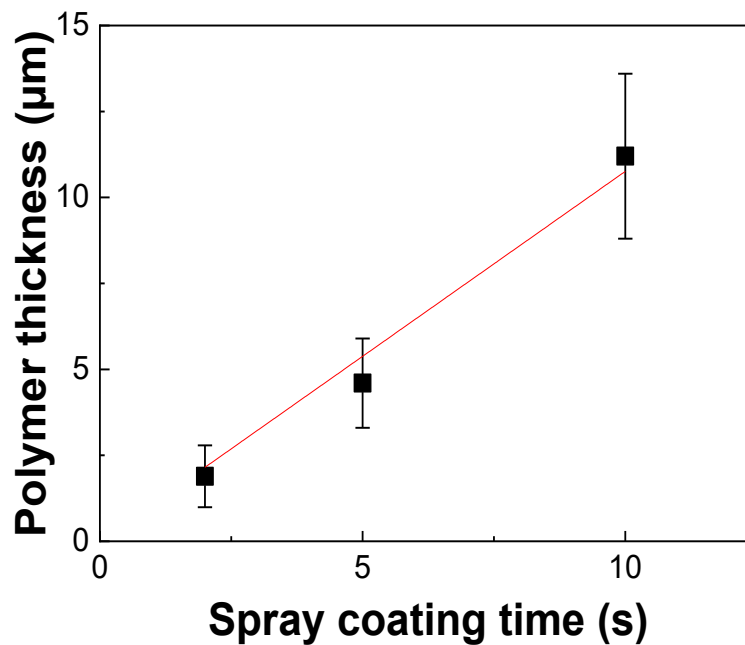


Figure 17. Protection layer thickness as a function of spray coating time. The linear equation for the coating rate was $y = 1.076 \cdot x$. Error bars indicate the standard deviation as calculated by the SEM analysis in Table 2.

Furthermore, the

5.5 Release Behavior of the Patch with a Protection Layer in Simulated Digestive Conditions of Poultry

To characterize the pH-dependent release behavior of the patch with different thicknesses of the S100 protection layer, time-dependent release tests were performed using SB dye-encapsulated patch (SB-patch) in simulated digestive conditions. For this purpose, SB-patches were initially exposed to the simulated gastric fluid (SGF; pH = 2.0, time: 45 min), followed by the simulated intestine fluid (SIF; pH = 7.1, time: 60 min). The release behavior was monitored by measuring fluorescence intensity during incubation in simulated digestive conditions.

As shown in Figure 18, all patch samples exhibited a gradual release over the course of incubation in SGF, followed by a rapid release upon exposure to SIF. For all samples, there was a significant increase in the fluorescence intensity upon exposure to the SIF at 45 min, which is also when the pH increased to 7.1. This would be expected, as the S100 polymer is known to dissolve in environments where the pH is greater than 7.

As Figure 19 shows, a higher level of encapsulated SB leakage in SGF was observed from the patch samples with the thinner passivation layer. Nearly 35% of the dye had been released by the end of the SGF incubation for the patches with 2 s of spray coating, whereas the 5-s and 10-s coating conditions had significantly lower amounts of dye released under the same conditions. Under different spray coating conditions, the release rate of SB in SGF was measured to be linearly correlated: $R = 0.841 \cdot t$ (2-s spray coating), $R = 0.568 \cdot t$ (5-s spray coating), $R = 0.251 \cdot t$ (10-s spray coating), where R is the percent dye released and t is the time exposed to the SGF in min (Figure 19). Using these experimental equations, the amount of dye released at the end of the SGF incubation was 34 ± 16 %, 23 ± 8 %, and 10 ± 8 % for 2-, 5-, and 10-s spray coated samples respectively. As shown in Figure 20, a clear decreasing linear relationship was observed in the

amount of dye that was released as the spray coating time increased. Thus, with an increase in spray coating time, there is an increase in polymer thickness and decrease in the amount of leakage of SB dye.

An interesting release profile is noted in Figure 18 b and c, where there is rapid release of the dye upon exposure to the simulated intestinal fluid, followed by a linear increase in the release after approximately 80 min. Dissolution and diffusion mechanisms of the polymers play a role in the release of dye from the system. The S100 polymer protects the system from the SGF, but upon exposure to the SIF, the rapid dissolution kinetics of the S100 polymer may explain the initial rapid release of dye. Then, as the CMC is exposed to the SIF, it likely swells and ultimately dissolves due to the chains disentangling, resulting in the zero-order release seen in the latter part of Figure 18 [69]. At this time, the dissolution rate may be dependent on the drug diffusion coefficient in the CMC [70]. Although it was not within the scope of the current research, further studies are needed to investigate the time-dependent release mechanism for target specific delivery of probiotics.

While not fully investigated in this work, leakage of the dye from the thin coating might be associated with defects of the coating or the leak of SB diffused into the passivation layer during the coating process. In addition, the conical structures of the samples could be affecting the dispersal of the polymer during the coating process, as the thickness of the polymer is likely lower on the side edges and base of the structure when compared to the tip. Thus, with an increase in spray coating time, the polymer thickness increases for all parts of the structure, minimizing the leakage, as seen for samples spray coated for 10 s. These findings support the idea that spray coating parameters can be adjusted to achieve time- and pH-dependent release of the model drug, SB dye, and that 10 s of spray coating produces a sufficient layer of the polymer to coat samples.

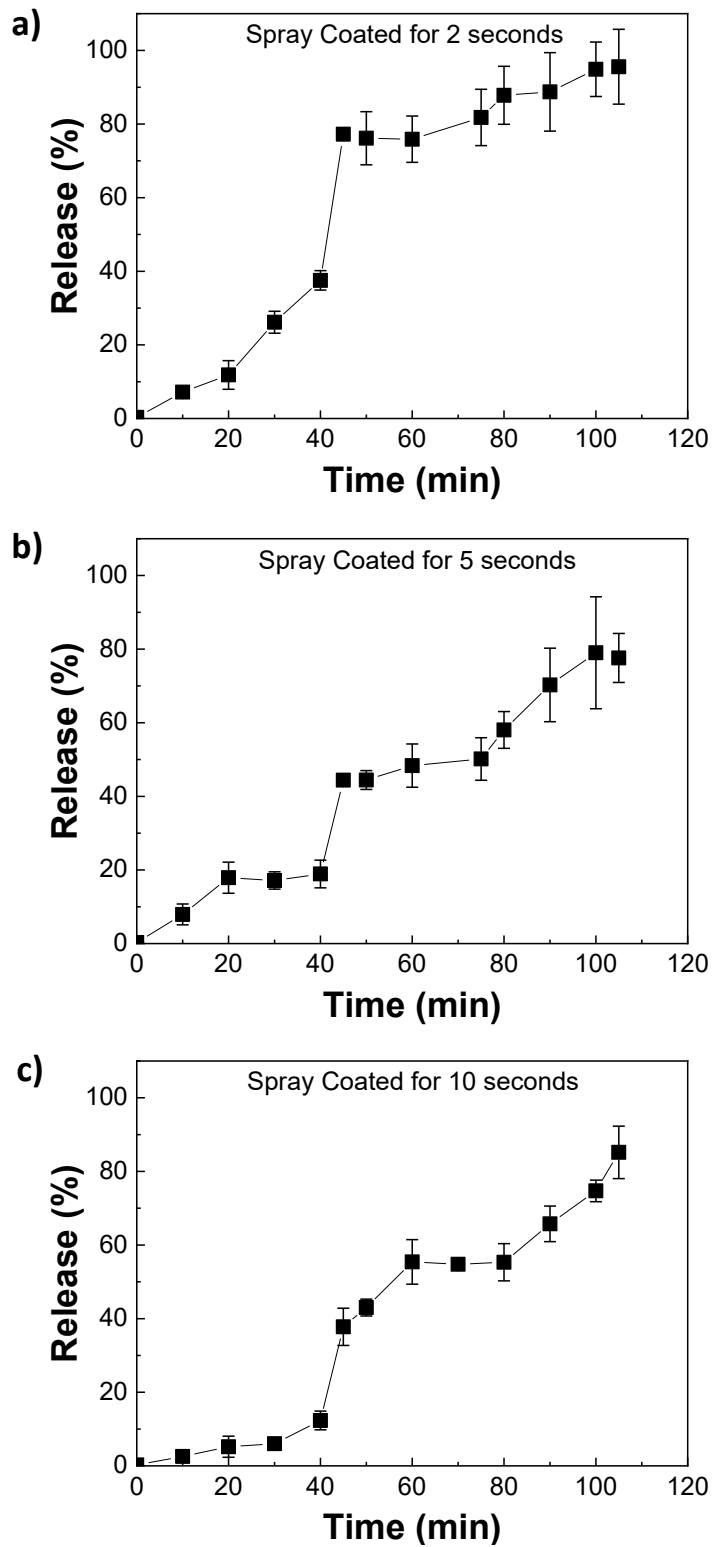


Figure 18. *In vitro* release test of SB dye encapsulated in molds spray coated for (a) 2 seconds, (b) 5 seconds, and (c) 10 seconds. The mean value was calculated from 3 replicates and the error bars indicate standard deviation.

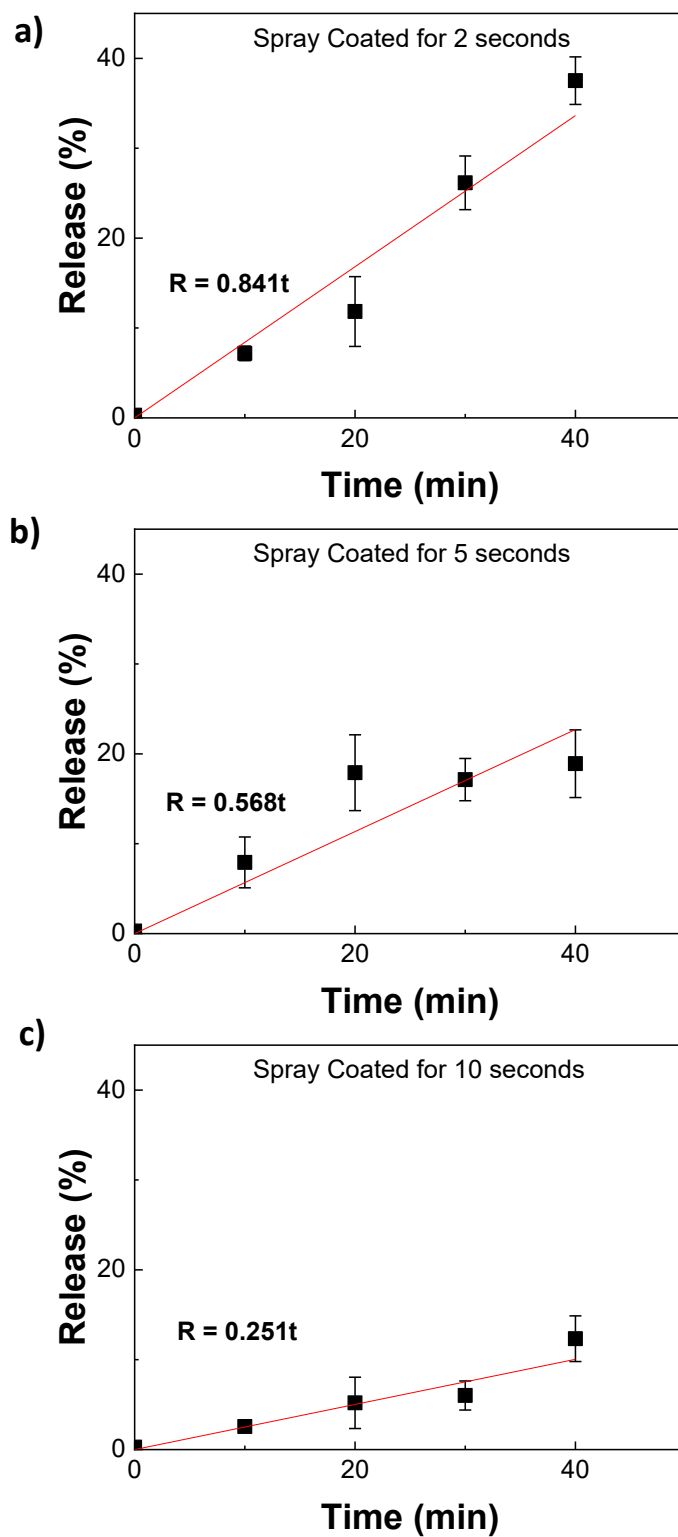


Figure 19. Release of SB dye as a function of time in SGF of molds spray coated for (a) 2 seconds, (b) 5 seconds, and (c) 10 seconds. The linear equation is seen on each plot, where R is the release rate (%) and t is the time exposed to SGF (min). The mean value was calculated from 3 replicates and the error bars indicate standard deviation.

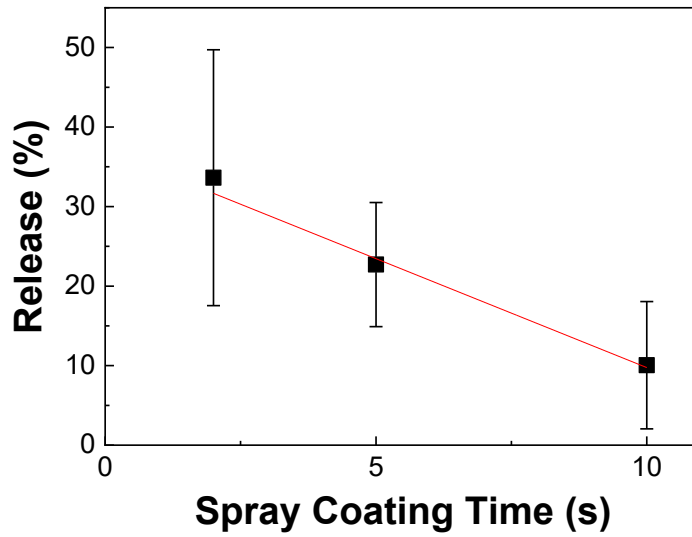


Figure 20. Release of SB dye in simulated gastric conditions as determined by experimental release rate equations for various periods of time a sample is spray coated. Error bars indicate the standard deviation as determined by the linear regression from Figure 19.

5.6 Preservation and Delivery of *L. acidophilus* in Simulated Digestive Conditions

The encapsulation efficiency of *L. acidophilus* in a single patch was determined to be $34.2 \pm 13.2 \mu\text{g}$. The time-dependent release behavior of a patch with encapsulated *L. acidophilus* exposed to simulated poultry digestive conditions is shown in Figure 21. All samples were demolded with a CMC backing, either with the S100 polymer protection layer (**Coated**) or without a protection layer (**Uncoated**). The CFU values were compared with those of 1) positive control samples, i.e. uncoated patch samples dissolved in DI (**Uncoated DI**), uncoated patch samples dissolved in PBS (**Uncoated PBS**), or coated patch samples exposed to SIF (**Coated intestine**), and 2) negative control samples, i.e. uncoated samples exposed to either SGF (**Uncoated stomach**) or exposed to SGF followed by SIF (**Uncoated digestive**). Notably, the positive controls, **Uncoated DI** and **Uncoated PBS**, did not show significant cell growth until 12 h of incubation in MRS, and it is only after 24 h of incubation that they exhibited a significant increase in CFU when compared to

the coated samples. In fact, 48-h incubation in MRS resulted in a similar cell viability for all positive controls compared to our sample. Thus, the addition of the S100 coating does not appear to cause negative impacts on the viability of the *L. acidophilus* cells. Moreover, due to the protection provided by the S100 coating, coated samples exhibited significantly higher levels of cell viability compared to the negative controls after 48 h of incubation in MRS. Furthermore, an increase in the cell viability between **Uncoated** _{stomach} and **Uncoated** _{digestive} was observed interestingly.

To eliminate the errors due to variations in the quantity of cells used in the procedures for the viability assays, a ratio can be applied to evaluate and compare between batches according to equation (1), where CFU/ protein is for the test condition of interest and CFU/ protein-DI is that of the **Uncoated** _{DI} sample:

$$\text{Relative CFU/ protein} = \frac{\text{CFU/ protein}}{\text{CFU/protein-DI}} \quad (1)$$

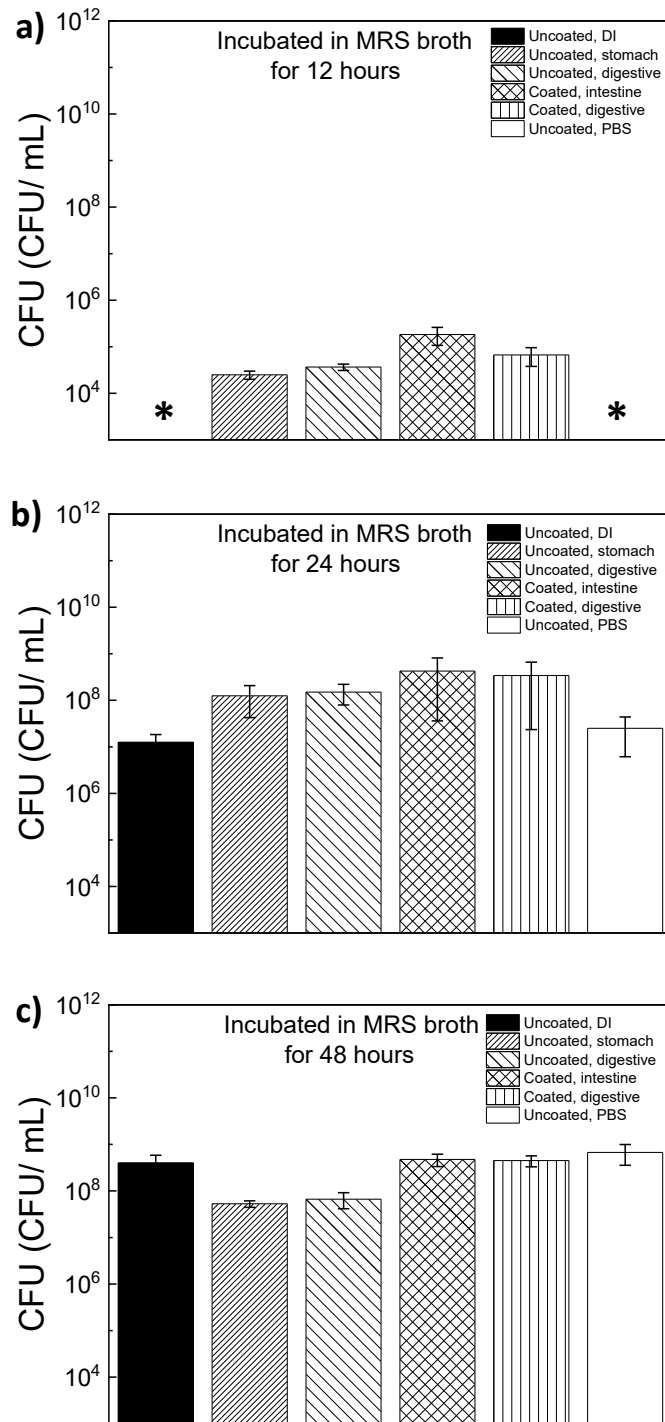


Figure 21. Time-dependent cell growth of *L. acidophilus* in simulated digestive conditions after incubation in MRS broth for (a) 12 hours, (b) 24 hours, and (c) 48 hours. Note: * CFU/mL < 500. The mean value was calculated from 3 replicates and the error bars indicate standard deviation.

As shown in Figure 22, it is clear that the variation in error increases upon combining the results from all three batches together. However, a significant difference is still seen in the *L. acidophilus* cell viability of our sample when compared to **Uncoated** _{stomach} and **Uncoated** _{digestive}. Thus, this further confirms that the S100 coating provides protection against the harsh digestive conditions. The batch-to-batch differences are most likely due to variations in the starting culture of cells and human error during the procedures. This can be further limited by increasing the batches tested. It is interesting to note that the **Uncoated** _{DI} samples did not show a significant difference in cell viability when compared to **Uncoated** _{PBS}. The **Uncoated** _{PBS} samples were measured to determine whether DI had any negative effects on the *L. acidophilus* cells, but as seen in Figure 22, that was not the case. Importantly, our coated patch samples showed 5.2 times greater cell viability after exposure to poultry digestive conditions when compared to samples without a protection layer. This significant improvement in the stability of the encapsulated cells can be advantageous in terms of dose sparing capabilities. That is, our probiotic formulation can exhibit the same level of therapeutic efficacy by using approximately 80% less cells compared to the conventional probiotics without protective formulations. Dose sparing is considered a key factor in pharmaceutical science, as pharmaceutical products often contain significantly more active products (in this case cells) than required. This is done in hopes of still achieving the targeted efficacy level even after cell loss due to exposure to harsh conditions. As mentioned previously, not only is this approach inefficient, but there are also concerns regarding the accuracy of dosages upon administration [71]. Having a platform that integrates the protection of cells during the formulation stages removes these hurdles that are often faced with drug delivery.

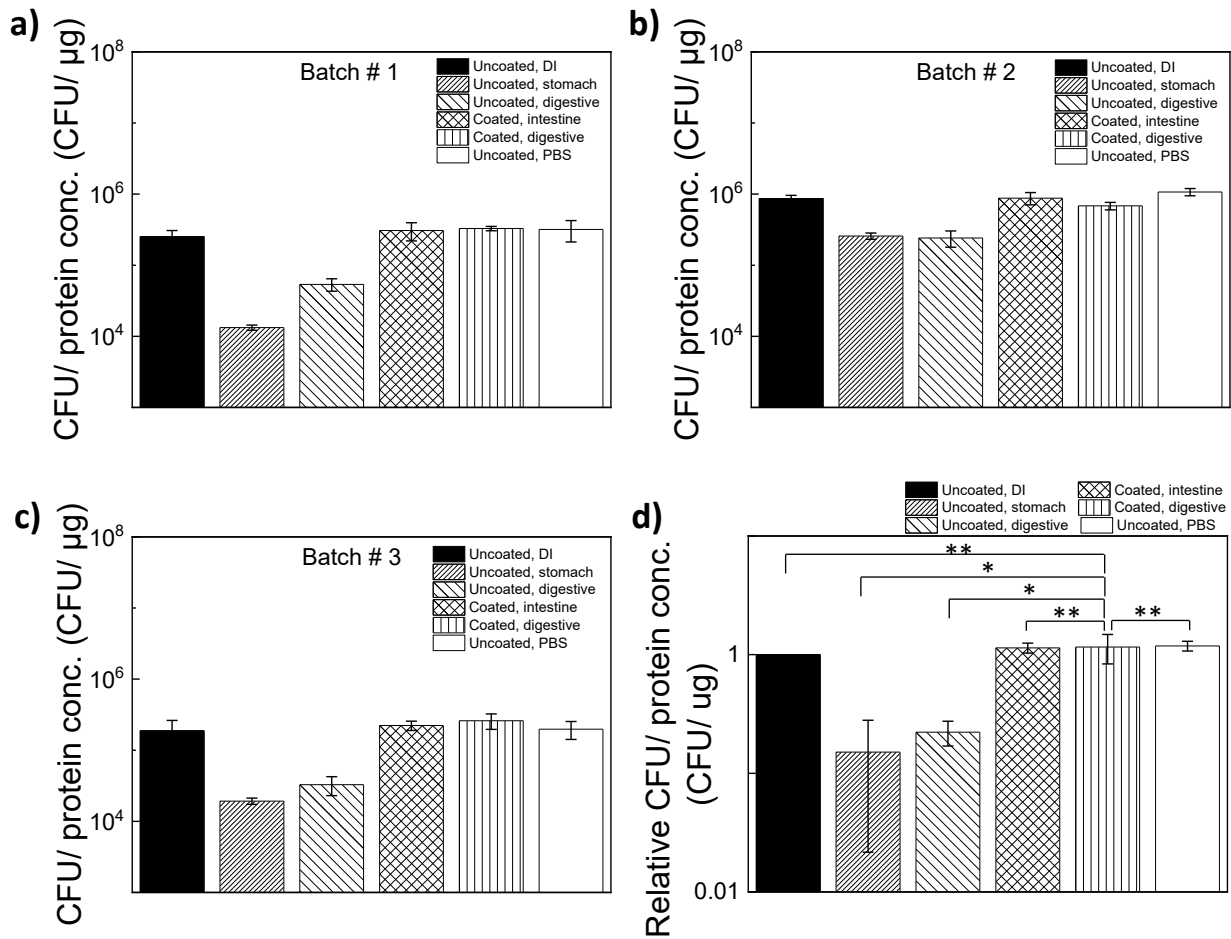


Figure 22. *L. acidophilus* cell viability after exposure to simulated digestive conditions and incubation in MRS broth for 48 hours. (a) Batch #1, (b) Batch #2, (c) Batch #3, and (d) all batches combined. The mean value was calculated from 3 replicates and the error bars indicate standard deviation for all except for (d) where the mean and standard deviation were calculated from the 3 batches. In Figure (d), * P < 0.05 and ** P > 0.05 by ANOVA.

To study the effects of antimicrobial substances produced from *L. acidophilus*, agar diffusion experiments were performed against *S. typhimurium*. Table 3 summarizes the sizes of the inhibition zones produced by each sample condition, indicating diffusion of antimicrobial substances through the agar. From the comparison of the diameter of the inhibition zones, it is observed that the antimicrobial activity of our coated patch sample was higher than that of the negative controls. This result is consistent with the cell viability data in digestive conditions

(Figure 22). It should be noted that some studies report potential antimicrobial activity from dead probiotic cells [56]. This may be the case for the negative controls in the present study, as it was shown previously that these had lower cell viability. Thus, the cell viability data should be taken in consideration with the agar well diffusion results to accurately understand what is occurring. An increased number of viable cells together with larger inhibition zones of our samples further supports the protective efficacy of the S100 polymer coating exposed to harsh environmental conditions.

Importantly, it should be noted that the organic solvent composition is a critical factor in determining the extent of solubility of the polymer and compatibility with the microfabrication of the probiotic formulations. In this work, we used the co-solvent, composed of dichloromethane:ethanol:isopropanol in a 2:1:1 ratio, that our group has previously applied for the fabrication of pH-responsive macropored microparticle's using microemulsion technology [72], [73]. It was found that the increase in the composition of dichloromethane makes it difficult to spray coat the polymer due to a rapid solvent evaporation and poor adhesion between polymer coating and trehalose. On the other hand, an increase in the composition of more polar solvents dissolve trehalose and damage encapsulated cells. Our application confirms that our co-solvent does not appear to destabilize the *L. acidophilus* cells while also maintaining the integrity of the microfabricated structures.

Table 3. Agar well diffusion inhibition zone produced by *L. acidophilus* against *S. typhimurium*. The mean value and standard deviation were calculated from 3 replicates.

Condition	Diameter (cm)
Uncoated _{DI}	2.72 ± 0.30
Uncoated _{stomach}	2.39 ± 0.15
Uncoated _{digestive}	2.41 ± 0.30
Coated _{intestine}	2.62 ± 0.19
Coated _{digestive}	2.64 ± 0.18
Uncoated _{PBS}	2.69 ± 0.14

5.7 Environmental Stability Test of *L. acidophilus*

The Food and Drug Administration (FDA) has a guideline for stability tests that should be conducted before application for a new drug product. These tests may, for example, quantify the degradability of a drug over time in various environmental conditions to evaluate the shelf life of the product [74]. The long-term stability of our formulation was tested by storing the samples at 37 °C and 70 % RH for 1 day vs. 1 week, in different packaging, sealed vs. unsealed, as seen in Table 4. For all conditions, the negative control was once again **Uncoated**_{digestive}. The stability of the formulations after storage and exposure to the simulated poultry digestive conditions is shown in Figure 23. As expected, the results support the observation that S100 polymer coating protects the *L. acidophilus* cells, as the cell viability is significantly higher for the coated samples in contrast to the uncoated samples. Additionally, the agar well diffusion inhibition diameters (Table 5) show that there was a difference in inhibition between all coated samples compared to the uncoated ones. The higher antimicrobial activity is likely due to the patch formulation with a protection layer

containing a significantly larger number of viable cells, thus enhancing the overall antimicrobial activity.

No significant difference was observed between the coated samples that were sealed or unsealed, meaning that the S100 polymer coating was well dispersed and has sufficient thickness to protect the samples against harsh environmental conditions. Moreover, the S100 polymer was protecting the cells from hydrolytic degradation, as it forms a barrier between the cells and the humidity in the environment; this was supported by the fact that the unsealed samples exposed to 70 % RH did not show significant difference in cell viability when compared to the sealed samples. Thus, not only was the S100 polymer coating protecting the cells against the harsh environmental conditions of the poultry digestive system, but it was also useful in protecting against the humidity in the environment during storage. This protective efficacy is a significant benefit for our formulation, as it has been shown that hydrolytic degradation often hinders the therapeutic benefits of drugs by reducing the stability during shelf life [75]. Yang et al. found that the S100 polymer is water insoluble due to the aggregated structure of the polymer chains, resulting in a water insoluble barrier [75]. Protection from hydrolytic degradation is therefore integrated into the formulation of our samples, minimizing the future need for extensive packaging of samples for protection during storage.

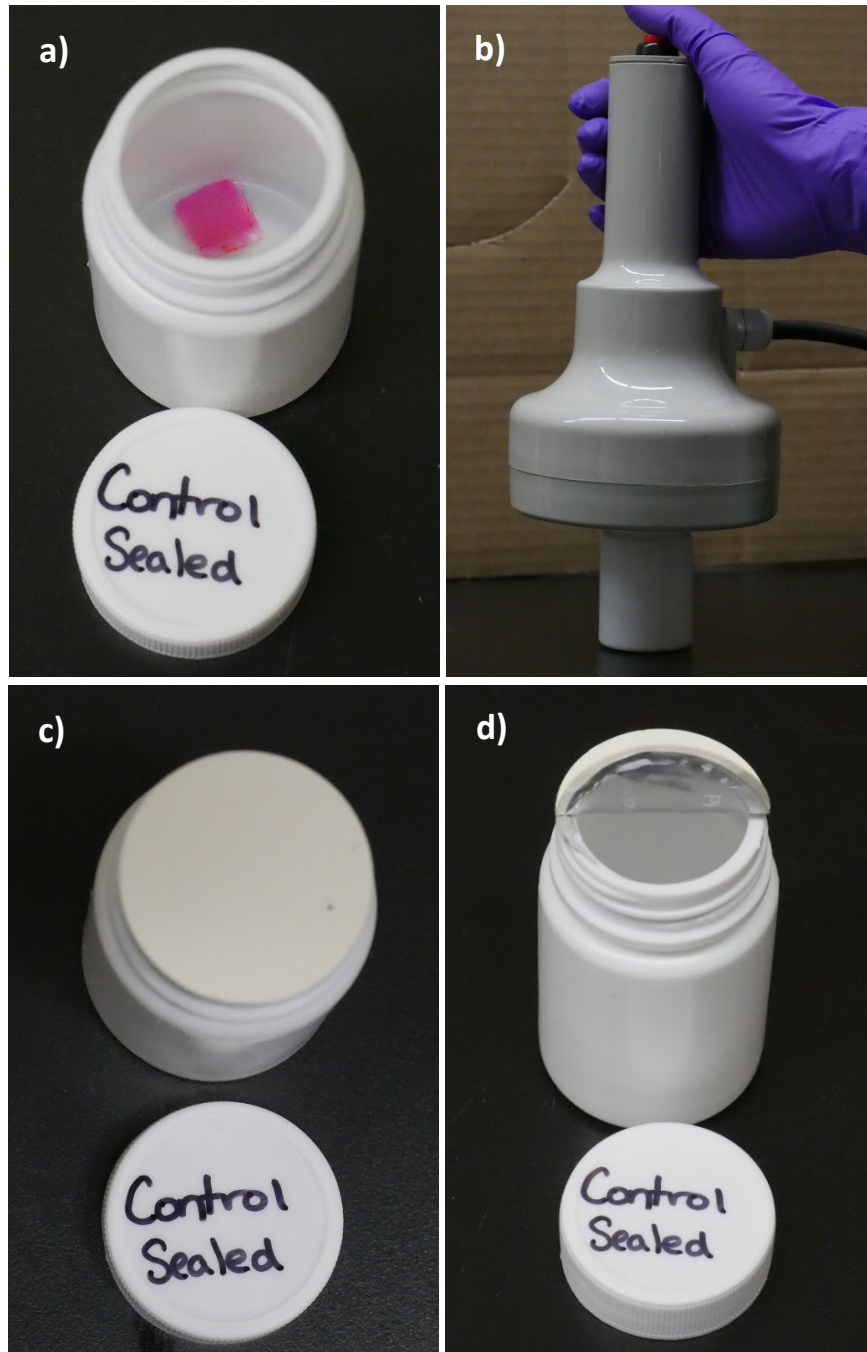


Figure 23. Sealing of samples for stability tests. (a) Patch encapsulated with SB dye in a pill bottle, (b) Sealing of bottles foil seal using electromagnetic induction sealer, (c) Visual confirmation of successful sealing of foil, and (d) Removal of foil seal from bottle.

A significant difference was seen between the sealed coated samples stored for 1 day when compared to those stored for 1 week. Similar results were found in literature, where Klayraung et al. noted that long-term storage of probiotic formulations at 30 °C caused a decrease in cell

viability, whereas storage at 10 °C did not [76]. Since a decrease in cell viability was seen, the process and formulation could be further optimized to further limit the degradation. Stability tests were only conducted under environmental conditions that would cause the most significant effect on cell viability (37 °C and 70 % RH), but further analysis could help to draw an appropriate conclusion.

Table 4. Environmental Stability Test Conditions

Storage	Sample	Testing	Label
Sealed	Spray coated	Digestive	Coated _{digestive-S}
	Bare	DI	Uncoated _{digestive-S}
Unsealed	Spray coated	Digestive	Coated _{digestive-U}
	Bare	DI	Uncoated _{digestive-U}

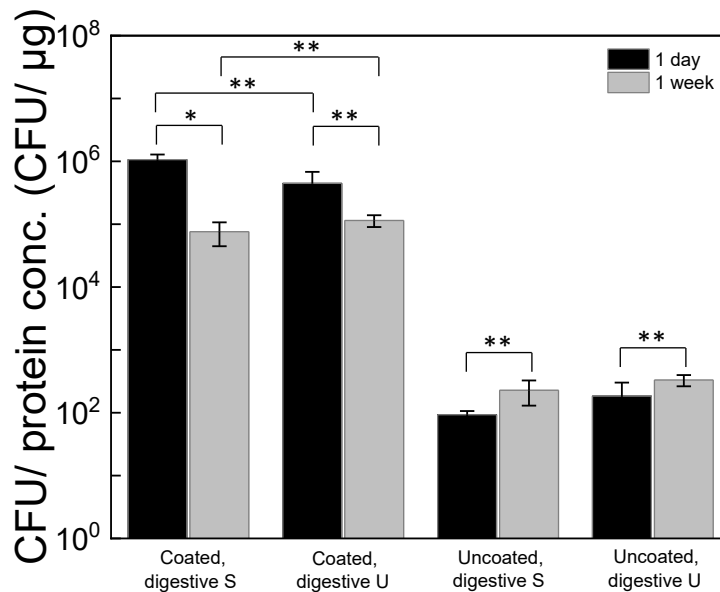


Figure 24. Environmental stability of cells upon exposure to digestive conditions after storage at 37 °C and 70 % RH for 1 day and 1 week. The mean value was calculated from 3 replicates and the error bars indicate standard deviation. * P < 0.05 and ** P > 0.05 by ANOVA.

Table 5. Agar well diffusion inhibition zone diameters for samples upon exposure to digestive conditions after being stored at 37 °C and 70 % RH for 1 day and 1 week. The mean value and standard deviation was calculated from 3 replicates.

Conditions	Diameter (cm)	
	1 day	1 week
Coated _{digestive-S}	4.85 ± 0.15	4.93 ± 0.28
Coated _{digestive-U}	5.21 ± 0.28	5.16 ± 0.41
Uncoated _{digestive-S}	3.30 ± 0.15	3.15 ± 0.12
Uncoated _{digestive-U}	3.68 ± 0.18	3.40 ± 0.38

6. Conclusions and Future Work

This study explored the integration of micromilling/ micro-molding technologies with drug delivery to produce a platform to encapsulate and deliver the probiotic *L. acidophilus*. Probiotics have been shown to reduce the virulence of various pathogens, such as *Salmonella*, in poultry, and provide other enhancements to poultry health – such as improvement in the growth of broiler chickens. They have been proposed as alternatives to antibiotics, especially recently with an increase in awareness of the significant negative impacts of antibiotics on both human and poultry health. The main goal was to develop a formulation that would protect the viability of the *L. acidophilus* cells against the harsh digestive conditions for targeted release in the poultry intestine.

A micromilling machine was used to successfully produce a 10×10 master mold on an aluminum plate for the fabrication of subsequent micro-sized systems using micro-molding concepts. Process parameters, such as vacuum oven cycles, centrifuge conditions, drying time, backing formulation, and spray coating thickness, were evaluated and optimized using SB dye as a model drug. Spray coating with S100 polymer was used to provide a protective barrier against

acidic environments, such as the low pH of the stomach of poultry. The release behavior was evaluated using SB dye to minimize leakage of the encapsulated agent, and pH-dependent release behavior was observed upon exposure to neutral conditions. Further analysis can be conducted regarding the impact of process parameters on the release behavior, such as optimization of spray coating for accurate time-dependent release. We were able to apply our findings from the successful demonstration of the encapsulation of our model drug, SB dye, to a real-life application with *L. acidophilus* cells.

The formulation and processing procedures developed were shown to have little to no negative effects on the viability of *L. acidophilus* cells. Moreover, *in vitro* tests with the S100 polymer coating proved to protect the cells in acidic environments, and allowed for the sustained release of cells upon exposure to the neutral conditions of the intestine, which was the targeted site for *L. acidophilus* release. A significant decrease in cell viability was noted for samples that were not coated with the S100 polymer and exposed to harsh digestive conditions, further showing the efficacy of the barrier. Larger inhibition zone diameters were seen with the use of the S100 polymer compared to no polymer, which was attributed to a higher number of viable cells after exposure to the digestive conditions. A lag was seen in the detection of viable cells when compared to a control. It was hypothesized to be due to viable but non-culturable cells in a dormant stage. To fully understand the behavior of the cells, further analysis can be conducted to confirm the metabolic state of the cells.

Storage stability tests were conducted to determine the degradation of the formulation under harsh storage conditions. The S100 polymer provided a barrier to protect the formulation against humidity in addition to its protective efficacy in digestive conditions. The polymer prevented hydrolytic degradation often seen with pharmaceutical drugs during storage due to

humidity. However, a decrease in cell viability was seen when stored for 1 week in comparison to 1 day, which was attributed to the formulation. For future work, the stability tests should be conducted for longer periods of time to understand the rate of degradation. This would also help in optimizing the process and formulation to minimize the degradation. Furthermore, other storage conditions should be tested, such as storage at 4 °C, which is also normal refrigerator temperatures.

Lastly, an important aspect of this work was utilizing geometric structures at the micron-scale to improve various aspects of drug delivery. With the proof-of-concept of encapsulation of a biological agent in this study, a natural next step would be to explore co-delivery abilities with the unique structure and properties of the current platform.

References

- [1] J. Davies and D. Davies, "Origins and Evolution of Antibiotic Resistance," *Microbiology and Molecular Biology Reviews*, vol. 74, no. 3, pp. 417-433, 2010.
- [2] Q. Chang, W. Wang, G. Regev-Yochay, M. Lipsitch and W. P. Hanage, "Antibiotics in agriculture and the risk to human health: how worried should we be?," *Evolutionary Applications*, vol. 8, no. 3, pp. 240-247, 2015.
- [3] D. V. T. Nair, K. Venkitanarayanan and A. K. Johny, "Antibiotic-Resistant Salmonella in the Food Supply and the Potential Role of Antibiotic Alternatives for Control," *Foods*, vol. 7, no. 10, p. 167, 2018.
- [4] T. Boeckel, C. Brower, M. Gilbert, B. Grenfell, S. Levin, T. Robinson, A. Teillant and R. Laxminarayan, "Global trends in antimicrobial use in food animals," *PNAS*, vol. 112, no. 18, pp. 5649-5654, 2015.
- [5] C. Manyi-Loh, S. Mamphweli, E. Meyer and A. Okoh, "Antibiotic Use in Agriculture and Its Consequential Resistance in Environmental Sources: Potential Public Health Implications," *Molecules*, vol. 23, no. 4, p. 795, 2018.
- [6] A. A. Velayati, M. R. Masjedi, P. Farnia, P. Tabarsi, J. Ghanavi, A. H. ZiaZarifi and S. E. Hoffner, "Emergence of New Forms of Totally Drug- Resistant Tuberculosis Bacilli," *CHEST*, vol. 136, no. 2, pp. 420-425, 2009.
- [7] K. L. Tang, N. P. Caffrey, D. B. Nobrega, S. C. Cork, P. E. Ronksley, H. W. Barkema, A. J. Polachek, H. Ganshorn, N. Sharma, J. D. Kellner and W. A. Ghali, "Restricting the use of antibiotics in food-producing animals and its associations with antibiotic resistance in food-producing animals and human beings: a systematic review and meta-analysis," *Lancet Planetary Health*, vol. 1, pp. 316-327, 2017.
- [8] C. f. D. C. a. Prevention, "Foodborne Germs and Illnesses," U.S. Department of Health & Human Services, 18 March 2020. [Online]. Available: <https://www.cdc.gov/foodsafety/foodborne-germs.html>. [Accessed April 2020].
- [9] P. Velge, A. Wiedmann, M. Rosselin, N. Abed, Z. Boumart, A. M. Chausse, O. Grepinet, F. Namdari, S. M. Roche, A. Rossignol and I. Virlogeux-Payant, "Multiplicity of Salmonella entry mechanisms, a new paradigm for Salmonella pathogenesis," *Microbiology Open*, vol. 1, no. 3, pp. 243-258, 2012.
- [10] K. H. Darwin and V. L. Miller, "Molecular Basis of the Interaction of Salmonella with the Intestinal Mucosa," *Clinical Microbiology Reviews*, vol. 12, no. 3, pp. 405-428, 1999.
- [11] R. A. Giannella, "Salmonella," in *Medical Microbiology 4th edition*, Galveston, TX, University of Texas Medical Branch at Galveston, 1996, p. Chapter 21.
- [12] P. A. Barrow and U. Methner, *Salmonella in Domestic Animals*, Croydon: CABI, 2013.

- [13] J. Hotinger and A. May, "Antibodies Inhibiting the Type III Secretion System of Gram-Negative Pathogenic Bacteria," *Antibodies*, vol. 9, no. 3, p. 35, 2020.
- [14] B. Coburn, I. Sekirov and B. Finlay, "Type III Secretion Systems and Disease," *Clin Microbiol Rev.*, vol. 20, no. 4, pp. 535-549, 2007.
- [15] E. Jennings, T. Thurston and D. Holden, "Salmonella SPI-2 Type III Secretion System Effectors: Molecular Mechanisms And Physiological Consequences," *Cell Host & Microbe*, vol. 22, no. 2, pp. 217-231, 2017.
- [16] J. Galan and H. Wolf-Watz, "Protein delivery into eukaryotic cells by type III secretion machines," *Nature*, vol. 444, pp. 567-572, 2006.
- [17] J. Berkes, V. K. Viswanathan, S. D. Savkovic and G. Hecht, "Intestinal epithelial responses to enteric pathogens: effects on the tight junction barrier, ion transport, and inflammation," *Gut*, vol. 52, pp. 439-451, 2003.
- [18] E. C. Boyle, J. L. Bishop, G. A. Grassl and B. B. Finlay, "Salmonella: from Pathogenesis to Therapeutics," *Journal of Bacteriology*, vol. 189, no. 5, pp. 1489-1495, 2007.
- [19] S. Foley, R. Nayak, I. Hanning, T. Johnson, J. Han and S. Ricke, "Population Dynamics of Salmonella enterica Serotypes in Commercial Egg and Poultry Production," *Appl Environ Microbiol*, vol. 77, no. 13, pp. 4273-4279, 2011.
- [20] P. Antunes, J. Mourao, J. Campos and L. Peixe, "Salmonellosis: the role of poultry meat," *Clinical Microbiology and Infection*, vol. 22, no. 2, pp. 110-121, 2016.
- [21] C. Loc-Carrillo and S. Abedon, "Pros and cons of phage therapy," *Bacteriophage*, vol. 1, no. 2, pp. 111-114, 2011.
- [22] R. Atternury, M. Van Bergen, F. Ortiz, M. Lovell, J. Harris, A. De Boer, J. Wagenaar, V. Allen and P. Barrow, "Bacteriophage Therapy To Reduce Salmonella Colonization of Broiler Chickens," *Public Health Microbiology*, vol. 73, no. 14, pp. 4543-4549, 2007.
- [23] D. Lin, B. Koskella and H. Lin, "Phage therapy: An alternative to antibiotics in the age of multi-drug resistance," *World J Gastrointest Pharmacol Ther*, vol. 8, no. 3, pp. 162-173, 2017.
- [24] K. Zbikowska, M. Michalczuk and B. Dolka, "The Use of Bacteriophages in the Poultry Industry," *Animals*, vol. 10, p. 872, 2020.
- [25] R. Fuller, "History and development of probiotics," in *Probiotics*, Springer, Dordrecht, 1992, pp. 1-8.
- [26] D. Mack, "Probiotics," *Can Fam Physician*, vol. 51, no. 11, pp. 1455-1457, 2005.
- [27] P. Mackowiak, "Recycling Metchnikoff: Probiotics, the Intestinal Microbiome and the Quest for Long Life," *Frontiers in Public Health*, vol. 1, no. 52, 2013.

- [28] A. Endo, Y. Tanizawa and M. Arita, "Isolation and Identification of Lactic Acid Bacteria from Environmental Samples," in *Lactic Acid Bacteria*, New York, NY, Humana Press, 2019, pp. 3-13.
- [29] M. P. Mokoena, "Lactic Acid Bacteria and Their Bacteriocins: Classification, Biosynthesis and Applications against Uropathogens: A Mini-Review," *Molecules*, vol. 22, no. 8, p. 1255, 2017.
- [30] G. P. A. Klein, C. Bonaparte and G. Reuter, "Taxonomy and physiology of probiotic lactic acid bacteria," *International Journal of Food Microbiology*, vol. 41, no. 2, pp. 103-125, 1998.
- [31] M. Bull, S. Plummer, J. Marchesi and E. Mahenthalingam, "The life history of *Lactobacillus acidophilus* as a probiotic: a tale of revisionary taxonomy, misidentification and commercial success," *FEMS Microbiology Letters*, vol. 349, no. 2, pp. 77-87, 2013.
- [32] L. De Vuyst and E. Vandamme, *BACTERIOCINS OF LACTIC ACID BACTERIA: Microbiology, Genetics and Applications*, Blackie Academic & Professional, 1994.
- [33] P. Markowiak and K. Slizewska, "Effects of Probiotics, Prebiotics, and Synbiotics on Human Health," *Nutrients*, vol. 9, no. 9, p. 1021, 2017.
- [34] A. Monteagudo- Mera, R. Rastall, G. Gibson, D. Charalampopoulos and A. Chatzifragkou, "Adhesion mechanisms mediated by probiotics and prebiotics and their potential impact on human health," *Applied Microbiology and Biotechnology*, vol. 103, no. 16, pp. 6463-6472, 2018.
- [35] A. Servin, "Antagonistic activities of lactobacilli and bifidobacteria against microbial pathogens," *FEMS Microbiology Reviews*, vol. 28, no. 4, pp. 405-440, 2004.
- [36] S. Todorov, "Bacteriocins from *Lactobacillus plantarum* – production, genetic organization and mode of action," *Brazilian Journal of Microbiology*, vol. 40, no. 2, pp. 209-221, 2009.
- [37] R. Palffy, R. Gardlik, M. Behuliak, L. Kadasi, J. Turna and P. Celec, "On the physiology and pathophysiology of antimicrobial peptides," *Molecular Medicine*, vol. 15, no. 1-2, pp. 51-59, 2008.
- [38] N. Mira, M. Teixeira and I. Sa-Correia, "Adaptive Response and Tolerance to Weak Acids in *Saccharomyces cerevisiae*: A Genome-Wide View," *OMICS: A Journal of Integrative Biology*, vol. 14, no. 5, 2010.
- [39] B. Cords, S. Burnett, J. Hilgren, M. Finley and J. Magnuson, "Sanitizers: Halogens, Surface- Active Agents, and Peroxides," in *Antimicrobials in Food*, Boca Raton, FL, Taylor & Francis Group, 2005, pp. 507-562.
- [40] J. Piard and M. Desmazeaud, "Inhibiting factors produced by lactic acid bacteria. 1. Oxygen metabolites and catabolism end-products," *Dairy Science and Technology*, vol. 71, no. 5, pp. 525-541, 1991.
- [41] S. Yadav and R. Jha, "Strategies to modulate the intestinal microbiota and their effects on nutrient utilization, performance, and health of poultry," *Journal of Animal Science and Biotechnology*, vol. 10, no. 2, 2019.

- [42] B. Svihus, "Function of the digestive system," *Journal of Applied Poultry Research* , vol. 23, no. 2, pp. 306-314, 2014.
- [43] M. Martinez- Haro, M. Taggart, A. Green and R. Mateo, "Avian Digestive Tract Simulation To Study the Effect of Grit Geochemistry and Food on Pb Shot Bioaccessibility," *Environmental Science & Technology*, vol. 43, no. 24, pp. 9480-9486, 2009.
- [44] Y. Nazir, S. Hussain, A. Hamid and Y. Song, "Probiotics and Their Potential Preventive and Therapeutic Role for Cancer, High Serum Cholesterol, and Allergic and HIV Diseases," *Food Microbiology*, 2018.
- [45] R. Huang, K. Wang and J. Hu, "Effect of Probiotics on Depression: A Systematic Review and Meta-Analysis of Randomized Controlled Trials," *Nutrients*, vol. 8, no. 8, p. 483, 2016.
- [46] B. Mohan, R. Kadirvel, A. Natarajan and M. Bhaskaran, "Effect of probiotic supplementation on growth, nitrogen utilisation and serum cholesterol in broilers," *British Poultry Science*, vol. 37, no. 2, pp. 395-401, 1996.
- [47] A. Panda, M. Reddy, S. Rama Rao and N. Praharaj, "Production performance, serum/ yolk cholesterol and immune competence of White Leghorn layers as influenced by dietary supplementation with probiotic," *Tropical Animal Health and Production* , vol. 35, pp. 85-94, 2003.
- [48] R. Khan and S. Naz, "The applications of probiotics in poultry production," *World's Poultry Science*, vol. 69, no. 3, pp. 621-632, 2019.
- [49] M. Govender, Y. Choonara, P. Kumar, L. du Toit, S. van Vuuren and V. Pillay, "A Review of the Advancements in Probiotic Delivery: Conventional vs. Non-conventional Formulations for Intestinal Flora Supplementation," *AAPS PharmSciTech*, vol. 15, no. 1, pp. 29-43, 2014.
- [50] L. Serna-Cock and V. Vallejo-Castillo, "Probiotic Encapsulation," *African Journal of Microbiology Research*, vol. 7, no. 40, pp. 4743-4753, 2013.
- [51] S. Leslie, E. Israeli, B. Lighthart, J. Crowe and L. Crowe, "Trehalose and Sucrose Protect Both Membranes and Proteins in Intact Bacteria during Drying," *Applied and Environmental Microbiology*, vol. 61, no. 10, pp. 3592-3597, 1995.
- [52] D. Semyonov, O. Ramon, Z. Kaplun, L. Levin- Brener, N. Gurevich and E. Shimoni, " Microencapsulation of Lactobacillus paracasei by spray freeze drying," *Food Research International* , vol. 43, no. 1, pp. 193-202, 2010.
- [53] H. Solanki, D. Pawar, D. Shah, V. Prajapati, G. Jani, A. Mulla and P. Thakar, "Development of Microencapsulation Delivery System for Long-Term Preservation of Probiotics as Biotherapeutics Agent," *Biomed Res Int*, vol. 2013, 2013.
- [54] C. Hill, F. Guarner, G. Reid, G. Gibson, D. Merenstein, B. Pot, L. Morelli, R. Canani, H. Flint, S. Salminen, P. Calder and M. Sanders, "The International Scientific Association for Probiotics and

- Prebiotics consensus statement on the scope and appropriate use of the term probiotic," *Nature Reviews Gastroenterology & Hepatology*, vol. 11, pp. 504-514, 2014.
- [55] d. Simone and Claudio, "The Unregulated Probiotic Market," *Clinical Gastroenterology and Hepatology*, vol. 17, no. 5, pp. 809-817, 2019.
- [56] C. Adams, "The probiotic paradox: live and dead cells are biological response modifiers," *Nutrition Research Reviews*, vol. 23, pp. 37-46, 2010.
- [57] C. Fox, J. Kim, L. Le, C. Nemeth, H. Chirra and T. Desai, "Micro/nanofabricated Platforms for Oral Drug Delivery," *J Control Release*, vol. 219, pp. 432-444, 2016.
- [58] D. Guckenberger, T. de Groot, A. Wan, D. Beebe and E. Young, "Micromilling: A method for ultra-rapid prototyping of plastic microfluidic devices," *Lab Chip*, vol. 15, no. 11, pp. 2364-2378, 2015.
- [59] S. Filiz, L. Xie, L. Weiss and O. Ozdoganlar, "Micromilling of microbarbs for medical implants," *International Journal of Machine Tools & Manufacture*, vol. 48, pp. 459-472, 2008.
- [60] S. Filiz, L. Xie, L. Weiss and O. Ozdoganlar, "Micromilling of microbarbs for medical implants," *International Journal of Machine Tools and Manufacture*, vol. 48, no. 3-4, pp. 459-472, 2008.
- [61] M. Hupert, W. J. Guy, S. Llopis, H. Shadpour, S. Rani, D. Nikitopoulos and S. Soper, "Evaluation of micromilled metal mold masters for the replication of microchip electrophoresis devices," *Microfluidics and Nanofluidics*, vol. 3, pp. 1-11, 2007.
- [62] B. Koch, I. Rubino, F.-S. Quan, B. Yoo and H.-J. Choi, "Microfabrication for Drug Delivery," *Materials*, vol. 9, p. 646, 2016.
- [63] V. Sommerfeld, M. Schollenberger, L. Hemberle and M. Rodehutsord, "Modification and application of an in vitro assay to examine inositol phosphate degradation in the digestive tract of poultry," *Journal of the Science of Food and Agriculture*, vol. 97, no. 12, pp. 4219-4226, 2017.
- [64] H. Naghili, H. Tajik, K. Mardani, S. Rouhani, A. Ehsani and P. Zare, "Validation of drop plate technique for bacterial enumeration by parametric and nonparametric tests," *Veterinary Research Forum*, vol. 4, no. 3, pp. 179-183, 2013.
- [65] P. Shokryazadan, C. C. Sieo, R. Kalavathy, J. B. Liang, N. Alitheen, M. Jahromi and Y. Ho, "Probiotic Potential of Lactobacillus Strains with Antimicrobial Activity against Some Human Pathogenic Strains," *BioMed Research International*, vol. 2014, 2014.
- [66] A. Garcia, "Anhydrobiosis in bacteria: From physiology to applications," *J. Biosci.*, vol. 36, no. 5, pp. 939-950, 2011.
- [67] C. Morgan, N. Herman, P. White and G. Vesey, "Preservation of micro-organisms by drying; a review," *J Microbiol Methods*, vol. 66, no. 2, pp. 183-193, 2006.

- [68] C. Davis, "Enumeration of probiotic strains: Review of culture-dependent and alternative techniques to quantify viable bacteria," *Journal of Microbiological Methods*, vol. 103, pp. 9-17, 2014.
- [69] R. Harland, A. Gazzaniga, E. Sangalli, P. Colombo and N. Peppas, "Drug/ Polymer Matrix Swelling and Dissolution," *Pharmaceutical Research*, vol. 5, no. 8, pp. 488-494, 1988.
- [70] B. Narasimhan and N. Peppas, "Molecular Analysis of Drug Delivery Systems Controlled by Dissolution of the Polymer Carrier," *Journal of Pharmaceutical Sciences*, vol. 86, no. 3, pp. 297-304, 1997.
- [71] K. Fenster, B. Freeburg, C. Hollard, C. Wong, R. Laursen and A. Ouwehand, "The Production and Delivery of Probiotics: A Review of a Practical Approach," *Microorganisms*, vol. 7, no. 3, p. 83, 2019.
- [72] B. Homayun, C. Sun, A. Kumar, C. Montemagno and H.-J. Choi, "Facile fabrication of microparticles with pH-responsive macropores for small intestine targeted drug formulation," *European Journal of Pharmaceutics and Biopharmaceutics*, vol. 128, pp. 316-326, 2018.
- [73] J. Lee, T. Park and H. Choi, "Development of oral drug delivery system using floating microspheres," *Journal of Microencapsulation*, vol. 16, no. 6, pp. 715-729, 1999.
- [74] U.S. Department of Health and Human Services Food and Drug Administration, "U.S. Food & Drug Administration," November 2003. [Online]. Available: <https://www.fda.gov/regulatory-information/search-fda-guidance-documents/q1ar2-stability-testing-new-drug-substances-and-products>. [Accessed July 2020].
- [75] Q. Yang, F. Yuan, L. Xu, Q. Yan, Y. Yang, D. Wu, F. Guo and G. Yang, "An Update of Moisture Barrier Coating for Drug Delivery," *Pharmaceutics*, vol. 11, no. 9, p. 436, 2019.
- [76] S. Klayraung, H. Viernstein and S. Okonogi, "Development of tablets containing probiotics: Effects of formulation and processing parameters on bacterial viability," *International Journal of Pharmaceutics*, vol. 370, no. 1-2, pp. 54-60, 2009.
- [77] W.-Y. Fung, H.-S. Lye, T.-J. Lim, C.-Y. Kuan and M.-T. Liong, "Roles of Probiotic on Gut Health," in *Probiotics Biology, Genetics and Health Aspects*, Springer, 2011, pp. 139-160.
- [78] A. Wesche, J. Gurtler, B. Marks and E. Ryser, "Stress, Sublethal Injury, Resuscitation, and Virulence of Bacterial Foodborne Pathogens," *Journal of Food Protection*, vol. 72, no. 5, pp. 1121-1138, 2009.